JOC*Article*

Abc Amino Acids: Design, Synthesis, and Properties of New Photoelastic Amino Acids

Robert F. Standaert*,† and Seung Bum Park*,‡

Life Sciences Division, Oak Ridge National Laboratory, PO Box 2008 MS 6123, Oak Ridge, Tennessee 37831-6123, and School of Chemistry, Seoul National University, Seoul 151-742, Korea

standaertrf@ornl.gov; sbpark@snu.ac.kr

Received April 11, 2006

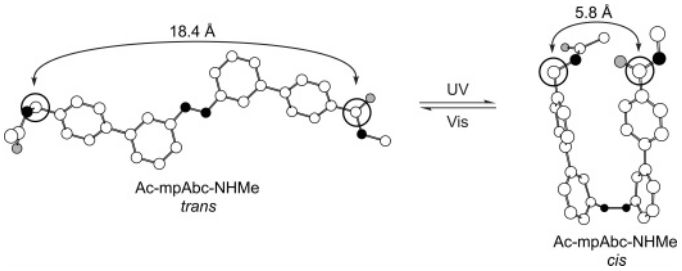

Photoisomerizable amino acids provide a direct avenue to the experimental manipulation of bioactive polypeptides, potentially allowing real-time, remote control of biological systems and enabling useful applications in nanobiotechnology. Herein, we report a new class of photoisomerizable amino acids intended to cause pronounced expansion and contraction in the polypeptide backbone, i.e., to be photoelastic. These compounds, termed Abc amino acids, employ a photoisomerizable azobiphenyl chromophore to control the relative disposition of aminomethyl and carboxyl substituents. Molecular modeling of nine Abc isomers led to the identification of one with particularly attractive properties, including the ability to induce contractions up to 13 Å in the backbone upon *trans* → *cis* photoisomerization. This isomer, designated mpAbc, has substituents at *meta* and *para* positions on the inner (azo-linked) and outer rings, respectively. An efficient synthesis of Fmoc-protected mpAbc was executed in which the biaryl components were formed via Suzuki couplings and the azo linkage was formed via amine/nitroso condensation; protected forms of three other Abc isomers were prepared similarly. An undecapeptide incorporating mpAbc was synthesized by conventional solid-phase methods and displayed characteristic azobenzene photochemical behavior with optimal conversion to the *cis* isomer at 360 nm and a thermal *cis* → *trans* half-life of 100 min at 80 °C.

Introduction

Many biologically important events depend on conformational changes that modulate the functions and interactions of proteins. Emulating this rapid, close coupling of changes in conformation to changes in function is a challenging goal for chemists, but one that promises great rewards in the development of new devices and biological tools. Light is an ideal agent for initiating conformational change in the biological context in that it can be delivered noninvasively, in precise quantity, and on an essentially instantaneous time scale, with wavelengths >300 nm being minimally absorbed by and having minimal effect on cells,[1] the obvious exception being those specifically responsive to light (e.g., melanocytes or photosynthetic cells). For these reasons, a significant body of work has emerged concerning the incorporation of organic photoswitches into peptide and protein systems to achieve robust photomodulation of function.[4]

Among photoswitches, the most popular choice in this context has been azobenzene (**1**), which undergoes reversible *cis*−*trans* isomerization of the N═N bond upon irradiation. The *trans* form is more stable by 49 kJ/mol[5] and as a consequence predominates to the virtual exclusion of the *cis* form at equilibrium (dark

† Oak Ridge National Laboratory.
‡ Seoul National University.

(1) Lester, H. A.; Nerbonne, J. M. *Annu. Rev. Biophys. Bioeng.* **1982**, *11*, 151−175.
(2) Bouwstra, J. A.; Schouten, A.; Kroon, J. *Acta Crystallogr., Sect. C* **1983**, *39*, 1121−1123.
(3) Mostad, A.; Rømming, C. *Acta Chem. Scand.* **1971**, *25*, 3561−3568.
(4) For a recent review, see: Renner, C.; Moroder, L. *ChemBioChem* **2006**, *7*, 869−878.

10.1021/jo060763q CCC: $33.50
Published on Web 09/12/2006

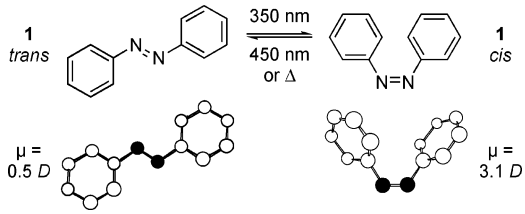

FIGURE 1. Photoisomerization of azobenzene. Conformations shown below the skeletal representations are taken from the X-ray crystal structures of *trans*[2] and *cis*[3] azobenzenes.

adaptation). Irradiation produces an excited state that partitions into a mixture of *cis* and *trans* isomers, and continuous irradiation leads to a photostationary state (PSS) in which the composition is governed by the concentrations (c), extinction coefficients (ϵ), and quantum yields (ϕ) for isomerization of the two isomers:[6]

$$c_c\epsilon_c\phi_{c\rightarrow t} = c_t\epsilon_t\phi_{t\rightarrow c} \quad (1)$$

As ϵ and to a lesser extent ϕ are wavelength-dependent, the PSS composition is also wavelength-dependent. Irradiation in the near UV (ca. 350 nm), where the *trans* has a higher extinction coefficient, produces a *cis*-rich mixture (typically 80−90% maximum), whereas irradiation in the visible region (ca. 450 nm), where the *cis* has a higher extinction coefficient, produces a mixture comparably enriched in *trans*. Irradiation at intermediate wavelengths produces mixtures of intermediate composition. These mixtures can be interconverted readily by irradiation at the appropriate wavelengths and persist for useful periods in the dark due to the absence of side reactions and slow rate of thermal isomerization ($t_{1/2}$ = 3.5 d for *cis* → *trans* isomerization of azobenzene in isooctane at 25 °C).[6] It is a fundamental property of the chromophore that irradiation always leads to mixtures. Though it is not possible to convert either isomer quantitatively into the other with light, it is possible to tune the isomer composition to any desired value between limiting extremes of typically 80−90% enrichment in either.

Photoisomerization (Figure 1) is accompanied by pronounced changes in conformation and dipole moment (0.5 D for *trans*, 3.1 D for *cis*[7]). Coupling these changes to functional changes in polypeptides has been pursued through three basic approaches. The first involves noncovalent association of a photoisomerizable modulating ligand with a polypeptide target. Notable successes in this approach include an azobenzene-based acetylcholine mimic, termed Bis Q (**2a**, Figure 2),[8] and azobenzene-based inhibitors of cysteine and serine proteases.[9] A photoactivated lipoxygenase inhibitor containing an alternative photoisomerizable chromophore (a hemithioindigo) has also been described.[10] Willner and Rubin reported an interesting form of noncovalent modification in which chymotrypsin was immobilized in photoresponsive polymers that regulated substrate access to the enzyme.[11]

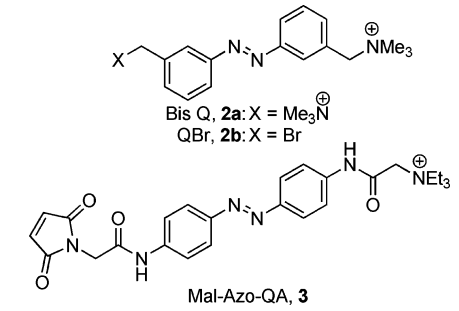

FIGURE 2. Structures of azobenzene-based ion-channel modulators.

The second approach involves covalent modification with azobenzene derivatives. An early success with this strategy was found with an analogue of Bis Q, QBr (**2b**), in which one end of the azobenzene is tethered to a trimethylammonio group that mimics acetylcholine and the other is tethered to a reactive benzylic bromide. This compound readily alkylates the nicotinic acetylcholine receptor after the native protein is treated with dithiothreitol, which reduces one or more disulfide bonds to expose reactive cysteine residues, leading to a light-responsive, modified receptor.[12] Recently, Banghart et al. successfully employed a variation of this approach with a potassium ion channel.[13] They likewise created a bifunctional azobenzene derivative (**3**) equipped with an reactive group and a channel-modulating group. In this instance, the maleimide function reacted with a specific cysteine residue introduced by site-directed mutagenesis, and the azobenzene controlled the presentation of a triethylammonio group, a mimic of the known channel blocker tetraethylammonium cation. Willner and coworkers were able to prepare a photomodulated derivative of the cysteine protease papain by acylation of surface amino groups with *p*-phenylazobenzoic acid.[14] A variety of azobenzene-containing derivatives of the pore-forming peptide antibiotic gramicidin have been created that display light-responsive ion conductivity in synthetic vesicles or bilayers. The first efforts involved N-terminal dimerization of the peptide through an intermediate azobenzene,[15] whereas more recent efforts have explored modifications of the C-terminus. Lien et al. used an azobenzene to alter the position of an ammonium group, which blocked the channel,[16] and Osman et al. used the azobenzene to position a carboxyl group, which influenced the peptide's

(5) Dias, A. R.; Minas da Piedade, M. E.; Simoes, J. A. M.; Simoni, J. A.; Teixeira, C.; Diogo, H. P.; Yang, M.; Pilcher, G. *J. Chem. Thermodyn.* **1992**, *24*, 439−447.

(6) Zimmerman, G.; Chow, L.-Y.; Paik, U.-J. *J. Am. Chem. Soc.* **1958**, *80*, 3528−3531.

(7) Bullock, D. J. W.; Cumper, W. W. N.; Vogel, A. I. *J. Chem. Soc.* **1965**, 5316−5323.

(8) (a) Bartels, E.; Wassermann, N. H.; Erlanger, B. F. *Proc. Natl. Acad. Sci. U.S.A.* **1971**, *68*, 1820−1823. (b) Nass, M. M.; Lester, H. A.; Krouse, M. E. *Biophys. J.* **1978**, *24*, 135−160. (c) Nargeot, J.; Lester, H. A.; Birdsall, N. J.; Stockton, J.; Wassermann, N. H.; Erlanger, B. F. *J. Gen. Physiol.* **1982**, *79*, 657−678. (d) Nerbonne, J. M.; Sheridan, R. E.; Chabala, L. D.; Lester, H. A. *Mol. Pharmacol.* **1983**, *23*, 344−349.

(9) (a) Kaufman, H.; Vratsanos, S. M.; Erlanger, B. F. *Science (Washington, D. C.)* **1968**, *162*, 1487−1489. (b) Westmark, P. R.; Kelly, J. P.; Smith, B. D. *J. Am. Chem. Soc.* **1993**, *115*, 3416−3419. (c) Harvey, A. J.; Abell, A. D. *Tetrahedron* **2000**, *56*, 9763−9771. (d) Harvey, A. J.; Abell, A. D. *Bioorg. Med. Chem. Lett.* **2001**, *11*, 2441−2444.

(10) Herre, S.; Schadendorf, T.; Ivanov, I.; Herrberger, C.; Steinle, W.; Rück-Braun, K.; Preissner, R.; Kuhn, H. *ChemBioChem* **2006**, *7*, 1089−1095.

(11) Willner, I.; Rubin, S. *React. Polym.* **1993**, *21*, 177−186.

(12) (a) Bartels, E.; Wassermann, N. H.; Erlanger, B. F. *Proc. Natl. Acad. Sci. U.S.A.* **1971**, *68*, 1820−1823 (b) Bartels-Bernal, E.; Rosenberry, T. L.; Chang, H. W. *Mol. Pharmacol.* **1976**, *12*, 813−819. (c) Lester, H. A.; Krouse, M. E.; Nass, M. M.; Wassermann, N. H.; Erlanger, B. F. *J. Gen. Physiol.* **1980**, *75*, 207−232.

(13) Banghart, M.; Borges, K.; Isacoff, E.; Trauner, D.; Kramer, R. H. *Nat. Neurosci.* **2004**, *7*, 1381−1386.

(14) Willner, I.; Rubin, S.; Riklin, A. *J. Am. Chem. Soc.* **1991**, *113*, 3321−3325.

(15) (a) Stankovic, C. J.; Heinemann, S. H.; Schreiber, S. L. *Biochim. Biophys. Acta* **1991**, *1061*, 163−170. (b) Sukhanov, S. V.; Ivanov, B. B.; Orekhov, S. Y.; Barsukov, L. I.; Arseniev, A. S. *Biol. Membr.* **1993**, *10*, 535−543.

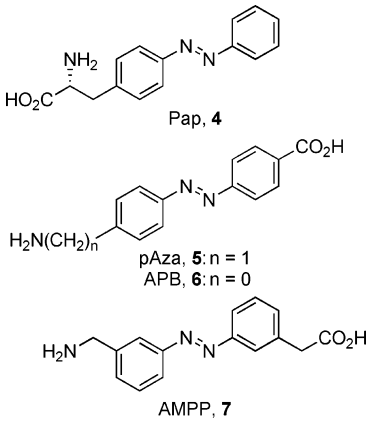

FIGURE 3. Structures of prototype azobenzene-based amino acids.

ability to insert into membranes.[17] Designed peptide nanopores have also been targeted via this approach. Ghadiri and co-workers used 4,4′-di(bromomethyl)azobenzene to dimerize a synthetic octapeptide via cysteine side chains and showed that photoisomerization caused a reversible conversion between intra- and intermolecularly hydrogen-bonded cylindrical structures.[18]

The third approach involves incorporation of a photoisomerizable amino acid directly into the polypeptide structure. In 1966, Goodman and Kossoy introduced *p*-phenylazophenylalanine (Pap, **4**, Figure 3),[19] the first amino acid bearing an intrinsic azobenzene functionality, which has subsequently been employed in the development of a variety of light-responsive polypeptides. Two groups have synthesized Pap-containing mutants of the ribonuclease S peptide that afforded photoregulation of ribonuclease activity upon complementation with the S protein.[20] Sisido and co-workers have expanded the scope of applications of Pap from chemically to biosynthetically produced polypeptides. Using a cell-free translation system, they substituted Pap into several positions of horseradish peroxidase (a 300-residue protein) and found that two of the mutants displayed photomodulated enzymatic activity.[21] Gramicidin has been targeted using the third approach as well as the second. Woolley and co-workers showed that gramicidin in which the N-terminal valine residue had been substituted with Pap[22] or a novel, photoisomerizable amino acid based on the hemithioindigo chromophore[23] formed photoresponsive ion channels in synthetic vesicles. In these instances, dipole effects were specifically linked to the changes in function, highlighting the importance of this property.

In 1994, Chmielewski introduced pAza (**5**),[24] the first amino acid in which the azobenzene resided within the backbone rather than in the side chain, and showed that it was able to modulate the conformation of a small cyclic peptide.[25] pAza was subsequently installed into a somatostatin analogue, where it induced a type II′ β-turn upon isomerization to the *cis* form, leading to enhanced affinity for the somatostatin receptor.[26] Moroder introduced a closely related amino acid, APB (**6**),[27] which differs only in lack of the benzylic methylene group, and has carefully investigated the conformational and photochemical properties of both APB and pAza in a number of cyclic peptides containing a fragment of the thioredoxin reductase active site,[28] the integrin-binding RGD motif,[29] and a peptide corresponding to the protein-disulfide isomerase (PDI) active site.[30] Important functional changes associated with photoisomerization included photomodulation of redox potential in the thioredoxin reductase peptides[31] and modulation of integrin binding in the RGD peptides. Two groups have independently designed and synthesized another related amino acid, AMPP (**7**), and demonstrated its ability to induce β-hairpin structures in model peptides upon photoisomerization.[32]

As these examples illustrate, azobenzene-based amino acids have proven themselves valuable reagents for the creation of polypeptides with light-modulated function. The potential for additional applications, combined with the limited number of available building blocks, has spurred the design and synthesis of new ones. We introduced phosphonic acid-bearing azobenzene-based amino acids,[33] Woolley and co-workers introduced a conformationally constrained azobenzene-based amino acid,[34] and Juodaityte and Sewald introduced two interesting azo-linked dimers of phenylalanine and *O*-methyltyrosine.[35] Additional amino acids based on alternative chromophores, such as the hemithioindigo, are also being developed rapidly.[22,36] In this report, we present our findings on the design of a new class of photoisomerizable amino acids along with the efficient synthesis and photochemical characterization of selected representatives.[37] Their general structure (Figure 4) is described by (aminomethyl)-

(16) Lien, L.; Jaikaran, D. C. J.; Zhang, Z. H.; Woolley, G. A. *J. Am. Chem. Soc.* **1996**, *118*, 12222−12223.
(17) Osman, P.; Martin, S.; Milojevic, D.; Tansey, C.; Separovic, F. *Langmuir* **1998**, *14*, 4238−4242.
(18) (a) Vollmer, M. S.; Clark, T. D.; Steinem, C.; Ghadiri, M. R. *Angew. Chem., Int. Ed.* **1999**, *38*, 1598−1601. (b) Steinem, C.; Janshoff, A.; Vollmer, M. S.; Ghadiri, M. R. *Langmuir* **1999**, *15*, 3956−3964.
(19) Goodman, M.; Kossoy, A. *J. Am. Chem. Soc.* **1966**, *88*, 5010−5015.
(20) (a) Liu, D.; Karanicolas, J.; Yu, C.; Zhang, Z. H.; Woolley, G. A. *Bioorg. Med. Chem. Lett.* **1997**, *7*, 2677−2680. (b) Hamachi, I.; Hiraoka, T.; Yamada, Y.; Shinkai, S. *Chem. Lett.* **1998**, 537−538.
(21) Muranaka, N.; Hohsaka, T.; Sisido, M. *FEBS Lett.* **2002**, *510*, 10−12.
(22) Borisenko, V.; Burns, D. C.; Zhang, Z. H.; Woolley, G. A. *J. Am. Chem. Soc.* **2000**, *122*, 6364−6370.
(23) Lougheed, T.; Borisenko, V.; Hennig, T.; Rück-Braun, K.; Woolley, G. A. *Org. Biomol. Chem.* **2004**, *2*, 2798−2801.
(24) Ulysse, L.; Chmielewski, J. *Bioorg. Med. Chem. Lett.* **1994**, *4*, 2145−2146.
(25) Ulysse, L.; Cubillos, J.; Chmielewski, J. *J. Am. Chem. Soc.* **1995**, *117*, 8466−8467.
(26) Ulysse, L. G., Jr.; Chmielewski, J. *Chem. Biol. Drug Des.* **2006**, *67*, 127−136.
(27) (a) Behrendt, R.; Renner, C.; Schenk, M.; Wang, F.; Wachtveitl, J.; Oesterhelt, D.; Moroder, L. *Angew. Chem., Int. Ed.* **1999**, *38*, 2771−2774. (b) Behrendt, R.; Schenk, M.; Musiol, H.-J.; Moroder, L. *J. Pept. Sci.* **1999**, *5*, 519−529.
(28) (a) Renner, C.; Behrendt, R.; Heim, N.; Moroder, L. *Biopolymers* **2002**, *63*, 382−393. (b) Renner, C.; Behrendt, R.; Spörlein, S.; Wachtveitl, J.; Moroder, L. *Biopolymers* **2000**, *54*, 489−500. (c) Renne, C.; Cramer, J.; Behrendt, R.; Moroder, L. *Biopolymers* **2000**, *54*, 501−514.
(29) (a) Schutt, M.; Krupka, S. S.; Milbradt, A. G.; Deindl, S.; Sinner, E. K.; Oesterhelt, D.; Renner, C.; Moroder, L. *Chem. Biol.* **2003**, *10*, 487−490. (b) Milbradt, A. G.; Löweneck, M.; Krupka, S. S.; Reif, M.; Sinner, E.-K.; Moroder, L.; Renner, C. *Biopolymers* **2005**, *77*, 304−313.
(30) Löweneck, M.; Milbradt, A. G.; Root, C.; Satzger, H.; Zinth, W.; Moroder, L.; Renner, C. *Biophys. J.* **2006**, *90*, 2099−2108.
(31) Cattani-Scholz, A.; Renner, C.; Cabrele, C.; Behrendt, R.; Oesterhelt, D.; Moroder, L. *Angew. Chem., Int. Ed.* **2002**, *41*, 289−292.
(32) (a) Aemissegger, A.; Kräutler, V.; van Gunsteren, W. F.; Hilvert, D. *J. Am. Chem. Soc.* **2005**, *127*, 2929−2936. (b) Kräutler, V.; Aemissegger, A.; Hünenberger, P. H.; Hilvert, D.; Hansson, T.; van Gunsteren, W. F. *J. Am. Chem. Soc.* **2005**, *127*, 4935−4942. (c) Dong, S. L.; Loweneck, M.; Schrader, T. E.; Schreier, W. J.; Zinth, W.; Moroder, L.; Renner, C. *Chem. Eur. J.* **2006**, *12*, 1114−1120.
(33) Park, S. B.; Standaert, R. F. *Tetrahedron Lett.* **1999**, *40*, 6557−6560.
(34) Zhang, J.; James, D. A.; Woolley, G. A. *J. Pept. Res.* **1999**, *53*, 560−568.
(35) Juodaityte, J.; Sewald, N. *J. Biotechnol.* **2004**, *112*, 127−138.
(36) (a) Steinle, W.; Ruck-Braun, K. *Org. Lett.* **2003**, *5*, 141−144. (b) Herre, S.; Steinle, W.; Rück-Braun, K. *Synthesis (Stuttgart)* **2005**, 3297−3300.

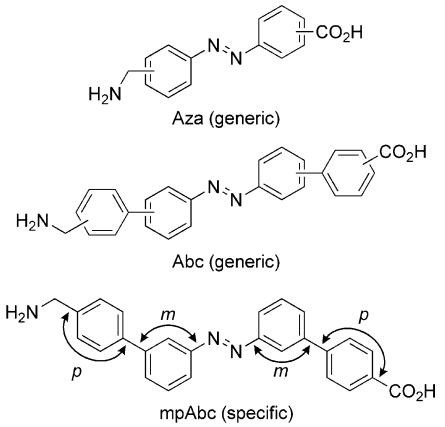

FIGURE 4. Comparison of Aza and Abc structures.

azobiphenylcarboxylic acid, which we abbreviate Abc. In descriptive terms, they are higher homologues of pAza in which azobiphenyl, rather than azobenzene, has been inserted between C and C_α of glycine with the aim of amplifying the photoelastic behavior (expansion, contraction, and distortion of the polypeptide backbone induced by photoisomerization) of pAza. This objective arose originally in connection with our efforts to generate light-regulated nuclear localization signal (NLS) peptides,[38] but we anticipate that Abc amino acids will be useful for a wide scope of other applications. Through molecular modeling, we were able to identify two isomers of Abc predicted to have significantly enhanced photoelastic behavior and focused our efforts on a single isomer, designated mpAbc (Figure 4), which became the main target for synthesis and photochemical characterization.

Results and Discussion

Design and Modeling of Abc Amino Acids. Our goal at the outset was, first, to analyze the conformational change that occurs upon photoisomerization of pAza and, second, to design and synthesize one or more new amino acids which would amplify the changes. The geometric change of most obvious consequence, and the one that is most predictable, is the change in the separation of the N- and C-terminal ends of the amino acid that occurs upon photoisomerization. We refer to the separation as the *span* (*R*) of the amino acid and the change in span as the *gating distance* (ΔR). The primary design goal for our purposes was one of maximizing gating distance, and we reasoned that extension of the azobenzene chromophore by a phenylene unit on either side would produce the desired result; the key remaining issue from the design perspective was the substitution pattern. For simplicity, we restricted our analysis to pseudosymmetric isomers (those which would be symmetrical about the azo linkage if the terminal attachments were identical). This restriction allows us to designate the three pseudo-symmetric Aza isomers by a single letter (o, m, or p) and the nine pseudo-symmetric Abc isomers by a two letter code (oo, om, etc), in which the first and second letters denote the substitution pattern on the inner rings and outer rings, respectively. For example, in mpAbc, the inner (azobenzene) rings have *meta* substituents and the outer rings have *para* substituents (Figure 4).

Molecular Modeling Overview. To identify isomers with enhanced gating distances, we initiated a molecular modeling study on pAza and the nine Abc isomers. All compounds were modeled as their N-terminal acetamide, C-terminal methylamide derivatives (Ac-Aza-NHMe or Ac-Abc-NHMe) to simulate the context of a polypeptide chain. Using MacroModel 6.0,[39] arbitrary starting conformations for the *cis* and *trans* isomers of each compound were created and energy-minimized using the supplied MM2* force field. Each starting structure was used to initiate a Monte Carlo search of 1000 new starting geometries, which were energy minimized to full convergence (energy gradient <0.01 kJ/Å) using the default PRCG (Polak-Ribiere conjugate gradient) algorithm. Smooth convergence required inclusion of all nonbonded interactions in the energy calculations, regardless of distance (BatchMin EXNB 3 command). Simulations employing the same starting geometry were performed without solvation (gas phase) and with GB/SA continuum-model solvation[40] by chloroform or water. To garner the maximum number of conformations, the output sets from each of the three simulations were merged and reminimized with the appropriate solvation model. Figure 5 shows the low-energy conformers from the water simulation for all nine Abc isomers as well as pAza. The number of unique conformations within 50 kJ/mol of the minimum for each Abc isomer ranged from a low of 48 for the *trans* form of the rigid pp isomer to 1132 for the *cis* form of the highly flexible mm isomer (Table 1).

It is clear from the number of conformers found that in most cases the searches were not exhaustive; however, they provide a sampling sufficient to identify the overall biases of the molecules and to identify major families of conformations. The conformers were analyzed on the basis of the span (*R*) between the carbonyl and methylene carbons as follows. For the *cis* and *trans* form of each compound, an energy-weighted average span was calculated, and the difference between these two averages was taken to be the effective gating distance, ΔR_{av}. An important caveat to the weighted-energy analysis is that its conclusions depend strongly on the accuracies of the molecular mechanics energies. Perhaps the greatest uncertainty lies in solvation, which was handled using a simple continuum model. Calculations with different solvent models generally led to similar conclusions, and the differences where noted were attributable to the dielectric constant. The water and chloroform solvation models uniformly compressed the distribution of observed energies, decreasing the bias introduced by the energy-weighting procedure. A second caveat is that the calculations do not consider the barriers between conformations. Although no indication of stable, alternative conformations was noted in NMR spectra of Abc derivatives, the possibility that pools of persistent conformers exist (alone or in the presence of a biomolecule) cannot be excluded.

Modeling of pAza. As pAza was the foundation for the design of new amino acids, it was important to investigate its properties at the outset. There are only five rotatable torsions

(37) Portions of this work have been previously disclosed: (a) Park, S. B. Ph.D. Thesis, Texas A&M University, 2001. (b) Park, S. B.; Standaert, R. F. *Abstracts of Papers*, 217th American Chemical Society Meeting, Anaheim, CA, 1999; American Chemical Society: Washington, DC, 1999; ORGN-094. (c) Park, S. B.; Standaert, R. F. *Abstracts of Papers*, 217th American Chemical Society Meeting, Anaheim, CA, 1999; American Chemical Society: Washington, DC, 1999; ORGN-097.

(38) Park, S. B.; Standaert, R. F. *Bioorg. Med. Chem.* **2001**, *9*, 3515−3523.

(39) Mohamadi, F.; Richards, N. G. J.; Guida, W. C.; Liskamp, R.; Lipton, M.; Caufield, C.; Chang, G.; Hendrickson, T.; Still, W. C. *J. Comput. Chem.* **1990**, *11*, 440−467.

(40) Still, W. C.; Tempczyk, A.; Hawley, R. C.; Hendrickson, T. *J. Am. Chem. Soc.* **1990**, *112*, 6127−6129.

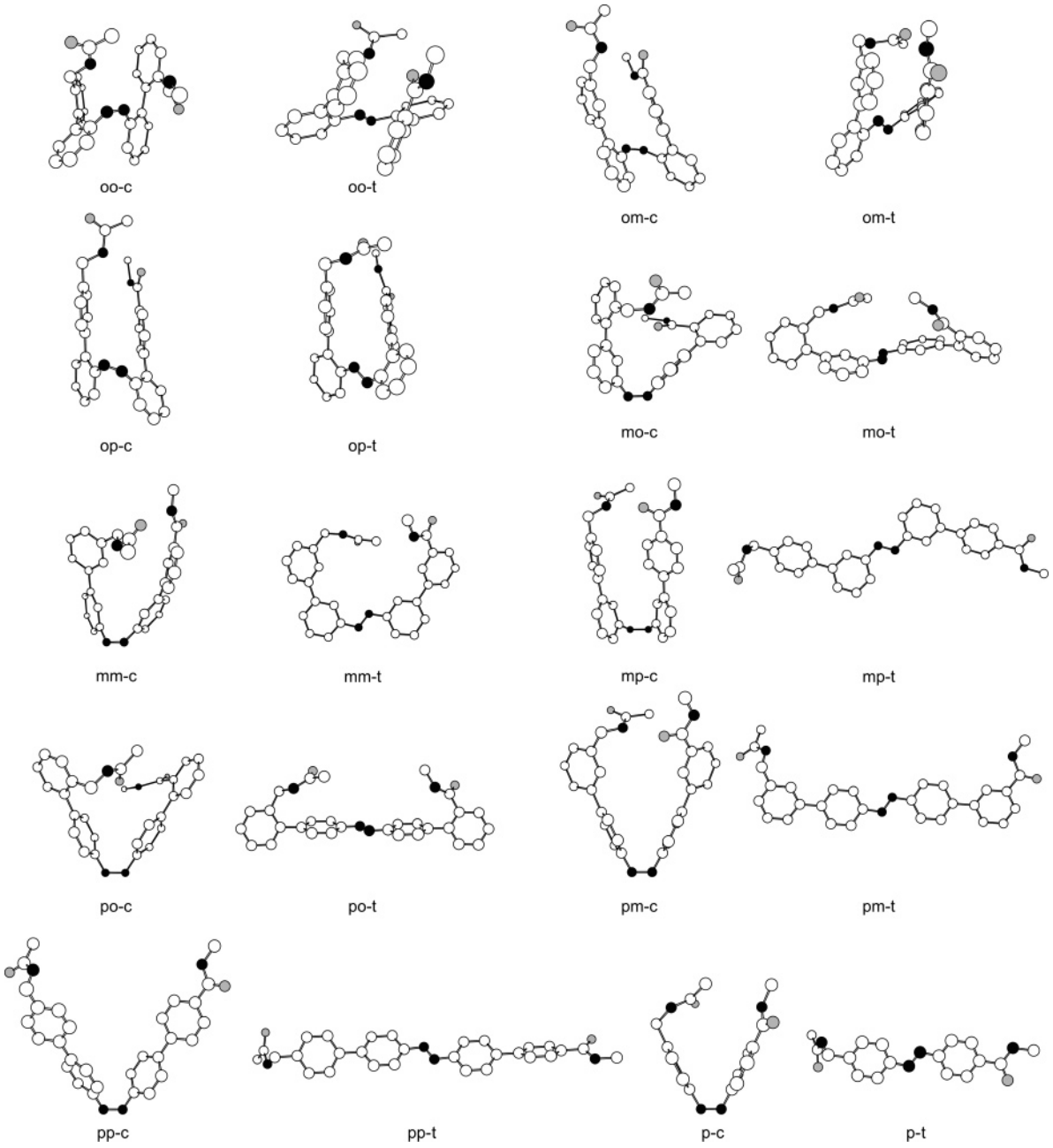

FIGURE 5. Low energy conformers of Ac-Abc-NHMe isomers and Ac-Aza-NHMe (lower right). The conformers shown are taken from Monte Carlo simulations with water solvation and are oriented such that the N-terminus is toward the left or upper left. Carbon atoms are uncolored, nitrogen atoms are black, oxygen atoms are shaded, and hydrogen atoms are not shown.

in the terminally capped derivative modeled, and to a first approximation, none of them affect span, making the analysis straightforward. Monte Carlo simulations with water solvation led to the identification of 16 unique conformers for *trans*-pAza and 23 for *cis*-pAza. Slightly fewer conformations were found in the gas-phase calculations for both isomers and in the chloroform calculation for *cis* (Table 1), perhaps reflecting strengthened electrostatic attractions in media of lower dielectric constant. In the *trans* conformers, the span is consistently 12.0 Å, and the azobenzene system is consistently planar. Planarity is to be expected because of the simple V2 potential specified in the MM2* force field for the aryl-azo bonds, though there is conflicting evidence regarding whether *trans* azobenzene is planar or slightly distorted from planarity. In the X-ray crystal structure of *trans* azobenzene,[2] the three observed conformers have C_i symmetry with the phenyl rings twisted 5−18° out of plane. Raman spectroscopy supports a C_i structure in solution,[42] whereas both gas-phase electron diffraction studies[43] and ab initio calculations[44] have produced conflicting conclusions. It is likely that the torsional potential near the planar structure is relatively flat, as was found in the calculations of Kurita et al.,[36d]

(41) Freund, J. E. *Modern Elementary Statistics*; 4 ed.; Prentice Hall: Englewood Cliffs, NJ, 1973.

(42) Kellerer, B.; Brandmul, J.; Hacker, H. H. *Indian J. Pure Appl. Phys.* **1971**, *9*, 903−909.

(43) (a) Traetteberg, M.; Hilmo, I.; Hagen, K. *J. Mol. Struct.* **1977**, *39*, 231−239. (b) Tsuji, T.; Takashima, H.; Takeuchi, H.; Egawa, T.; Konaka, S. *J. Phys. Chem. A* **2001**, *105*, 9347−9353.

TABLE 1. Summary of Spans (R) and Gating Distances (ΔR_{av}) for pAza and Abc Isomers

		n^b		R_{min} (Å)		R_{max} (Å)		$R_{av} \pm s_R$ (Å)^c		
compd	solv[a]	*cis*	*trans*	*cis*	*trans*	*cis*	*trans*	*cis*	*trans*	ΔR_{av} (Å)
pAza	g	18	12	5.39	11.99	7.68	12.00	6.19 ± 0.09	11.99 ± 0.00	5.80
	c	23	12	6.24	12.00	7.83	12.01	6.35 ± 0.34	12.00 ± 0.00	5.65
	w	23	16	6.32	11.99	7.47	12.00	6.84 ± 0.52	12.00 ± 0.00	5.16
mmAbc	g	854	652	3.50	5.05	15.63	18.02	4.49 ± 0.56	6.13 ± 1.14	1.64
	c	1132	644	3.63	5.14	15.93	18.04	4.68 ± 0.73	11.45 ± 4.31	6.77
	w	1017	662	3.56	5.14	15.47	18.03	5.20 ± 1.15	11.65 ± 3.63	6.45
moAbc	g	544	345	3.34	4.20	11.59	13.23	4.94 ± 0.53	5.67 ± 0.64	0.73
	c	649	423	3.50	4.24	11.97	13.29	5.08 ± 0.50	7.10 ± 2.27	2.02
	w	621	443	3.44	4.75	10.99	13.26	5.27 ± 1.09	8.54 ± 1.62	3.27
mpAbc	g	268	192	3.66	13.26	16.93	18.96	5.49 ± 0.77	15.78 ± 2.54	10.29
	c	372	192	3.89	13.32	17.27	18.97	5.84 ± 1.00	15.83 ± 2.54	9.98
	w	379	233	3.71	13.33	16.76	18.96	5.79 ± 1.35	15.67 ± 2.52	9.88
omAbc	g	546	588	3.38	3.41	12.97	13.50	4.24 ± 0.31	5.11 ± 0.43	0.87
	c	689	651	3.45	3.48	12.93	13.53	4.40 ± 0.45	5.13 ± 0.51	0.73
	w	680	713	3.45	3.57	12.99	13.50	4.93 ± 1.58	5.70 ± 1.11	0.77
ooAbc	g	284	296	3.43	3.44	9.98	9.49	4.87 ± 0.48	4.56 ± 0.30	−0.31
	c	296	312	3.46	3.82	9.98	10.07	5.03 ± 0.67	4.62 ± 0.30	−0.41
	w	342	384	3.48	3.69	10.11	9.89	6.36 ± 0.84	5.28 ± 0.77	−1.08
opAbc	g	148	146	3.43	3.61	12.26	13.58	4.71 ± 0.46	4.82 ± 0.47	0.11
	c	202	176	3.49	3.66	12.76	13.62	4.89 ± 0.52	5.09 ± 0.47	0.19
	w	219	200	3.50	3.63	12.28	13.58	5.21 ± 2.18	5.16 ± 0.77	−0.05
pmAbc	g	347	192	3.49	17.66	14.51	18.65	5.21 ± 0.63	18.07 ± 0.29	12.86
	c	418	192	4.02	17.68	14.78	18.66	5.83 ± 1.61	18.08 ± 0.29	12.25
	w	423	192	3.67	17.67	14.39	18.65	6.67 ± 2.21	18.07 ± 0.29	11.40
poAbc	g	184	86	3.58	12.00	11.72	13.45	5.76 ± 0.87	12.64 ± 0.44	6.87
	c	208	96	3.75	12.15	11.88	13.50	5.75 ± 0.81	12.75 ± 0.41	7.00
	w	216	112	3.56	12.09	11.62	13.47	6.01 ± 1.01	12.70 ± 0.42	6.69
ppAbc	g	96	48	11.00	20.65	12.32	20.66	11.98 ± 0.23	20.65 ± 0.00	8.67
	c	96	48	12.35	20.67	12.57	20.67	12.47 ± 0.05	20.67 ± 0.00	8.19
	w	123	58	11.89	20.65	12.06	20.66	11.99 ± 0.04	20.66 ± 0.00	8.67

[a] Solvent model employed: g, gas phase (vacuum); c, chloroform; w, water. [b] Number of unique conformers identified within 50 kJ/mol of the minimum. [c] The mean and standard deviation are weighted to reflect the population of each of the n conformers.[41] Thus, a normalized weight $w = c \exp(-\Delta E/RT)$ was assigned to each conformer, with the normalization constant c being such that $\sum w = n$. The mean distance is given by $R_{av} = \sum Rw/\sum w$, and the standard deviation is given by $s_R = \{[n(\sum R^2 w) - (\sum Rw)^2]\}/[n(n-1)]\}^{1/2}$.

who predicted that planar conformation is an energy maximum but lies only 1.5 kJ/mol above C_i minima with both rings twisted ±18° out of plane and that increasing the twist of both rings to 35° led to an energy only 3.1 kJ/mol above the minimum.

In the *cis* conformers of pAza, the azobenzene system adopts a conformation very similar to the C_2-symmetric structure observed in the X-ray crystal structure of *cis* azobenzene,[3] with both isomers having the aryl rings twisted substantially out of the C−N═N plane. Superposition of the low energy conformer of *cis* pAza (water solvation) on the crystal structure of azobenzene shows good overall agreement between the calculated and observed conformations (Figure 6), with an RMS deviation of 0.5 Å for all corresponding, non-hydrogen atoms. Two slight distortions are apparent. First, the phenyl rings in pAza are twisted further out of the N═N−C plane (57° X-ray, 72° modeling), and second, they are inclined more toward each other (C4−C4′ distance 6.16 Å in the X-ray structure, 5.18 Å in the modeled structure). When *cis* azobenzene itself is modeled, the overall agreement is excellent. The RMS deviation in position among non-hydrogen atoms is <0.2 Å, and the 57° phenyl ring twist of the X-ray structure is reproduced within 1°, suggesting that the additional ring twist in pAza is induced by interactions between terminal substituents. The phenyl rings are still inclined more toward each other than in the X-ray structure, though to a lesser extent than in pAza (C4−C4′ distance 5.76 Å). Close examination of the two structures reveals

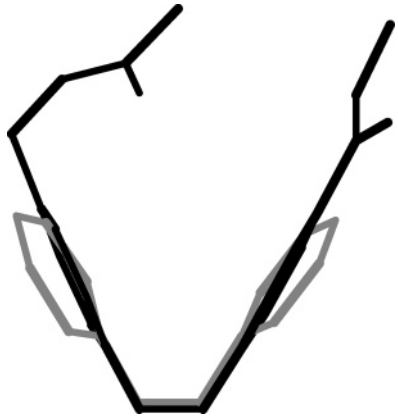

FIGURE 6. Modeled conformation of *cis* Ac-pAza-NHMe (black, N-terminus at upper left) superimposed on the crystal structrue of *cis* azobenzene (gray). Superimposition was performed using all non-hydrogen atoms of azobenzene and their counterparts in the pAza derivative.

(44) (a) Armstrong, D. R.; Clarkson, J.; Smith, W. E. *J. Phys. Chem.* **1995**, *99*, 17825−17831. (b) Biswas, N.; Umapathy, S. *J. Phys. Chem. A* **1997**, *101*, 5555−5566. (c) Hättig, C.; Hald, K. *Phys. Chem. Chem. Phys.* **2002**, *4*, 2111−2118. (d) Kurita, N.; Ikegami, T.; Ishikawa, Y. *Chem. Phys. Lett.* **2002**, *360*, 349−354. (e) Fliegl, H.; Kohn, A.; Hattig, C.; Ahlrichs, R. *J. Am. Chem. Soc.* **2003**, *125*, 9821−9827. (f) Tiago, M. L.; Ismail-Beigi, S.; Louie, S. G. *J. Chem. Phys.* **2005**, *122*, 094311.

that the C−N═N bond angles are identical, but in the X-ray structure the C−N bonds are bent slightly out of the ring planes (improper dihedral at C1/C1′ of 173°), tipping the rings away from each other and widening the molecule. This slight deviation from ideality is not reproduced in the calculated structure, which has in-plane C−N bonds. Among the modeled structures of pAza, the inclination of the rings toward each other is more pronounced than in the modeled structure of azobenzene, and it increases as the solvent polarity decreases (C4−C4′ distances 5.18, 5.07, and 4.94 Å for water, chloroform, and vacuum, respectively), suggesting that electrostatic attraction between the terminal substituents is responsible. The compression occurs mostly through reduction of the C−N═N bond angle, along with slight pyramidalization at C1/C1′, and causes a corresponding reduction of span in the *cis* conformers (6.32, 6.24, and 5.39 Å for water, chloroform, and gas-phase calculations, respectively).

Modeling of Abc Amino Acids. Molecular mechanics calculations on pAza predicted uniform spans among *cis* (6.2 Å) and *trans* (12.0 Å) conformers, such that the derived gating distance of 5.8 Å is well defined and provides a clear benchmark for new amino acids. As the calculated geometries of the azobenzene system reproduced experimental conformations with acceptable accuracy, we were encouraged to proceed with analogous calculations on Abc isomers. The low energy conformers for *cis* and *trans* forms of each Abc isomer and pAza, as found in the calculation with water solvation, are shown in Figure 5.

One concept that helps unify the results is that *para*-substitution leads to a rigid, rodlike structure, whereas *ortho*- and *meta*-substitution provide articulations that lead to greater flexibility and greater numbers of conformations. The properties of ppAbc directly mirror those of pAza. Like pAza, ppAbc has relatively few conformations, and as the allowed single-bond rotations have no effect on span, the spans (12.2 Å for *cis*, 20.7 Å for *trans*) and gating distance (8.5 Å) are values of precise meaning. An important conclusion is that ppAbc offers only a modest 2.7 Å improvement in gating distance over pAza. For the *trans* forms of both pAza and ppAbc, all conformers are essentially isoenergetic, differing by less than 1 kJ/mol regardless of solvent model. In the *cis* isomers, electrostatic effects and hydrogen bonding have a discernible influence on the calculated energies, particularly in pAza, where the termini are closer. In water, where electrostatic effects are attenuated, the conformers have similar energies (within 5.7 kJ/mol for pAza, 1 kJ/mol for ppAbc). In chloroform or the gas phase, pAza is predicted to have only two low-energy conformers, nearly isoenergetic with each other but 10 or 15 kJ/mol, respectively, more stable than the next most stable conformer. The factor governing this high stability appears to be the formation of a strong hydrogen bond between the terminal substituents in the low-energy conformers. In *cis* ppAbc, where hydrogen bond formation is not geometrically feasible, the energy differences are smaller (all conformers within 1.4 kJ/mol in chloroform, 2.5 kJ/mol in the gas phase).

For all other isomers, the gating distance is not precisely interpretable in terms of individual conformers; rather, it is the difference between two weighted averages. All of the oxAbc isomers (i.e., those with *ortho* substitution on the inner rings) have gating distances of 0 ± 1 Å. In these compounds, both *cis* and *trans* isomers display a strong preference for compact, folded forms with the terminal substituents in close proximity

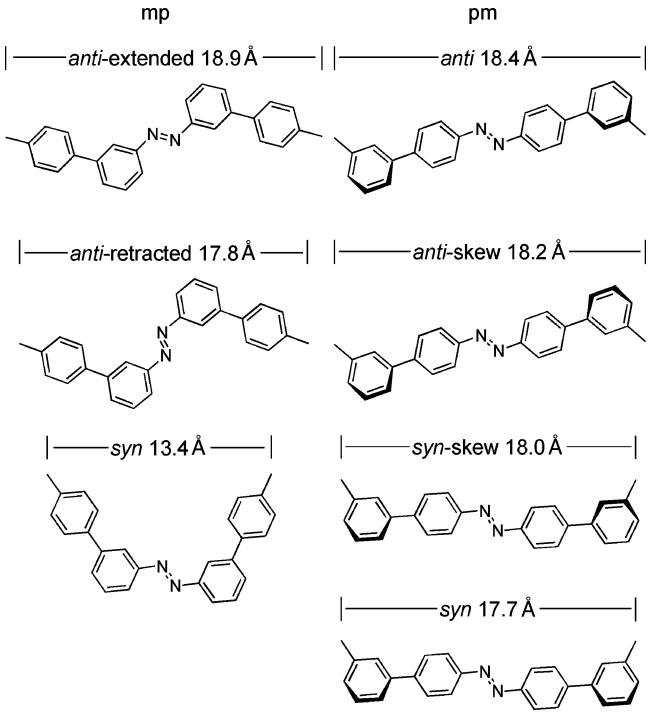

FIGURE 7. Azobiphenyl conformations in *trans* mpAbc and pmAbc.

(4−6 Å) regardless of solvation model. A small gating distance of ca. 2 ± 1 Å was also predicted for moAbc; in this compound, the structures calculated for the gas phase have uniformly smaller spans and lead to a predicted gating distance of only 0.73 Å, again reflecting the importance of electrostatics. Two compounds have predicted gating distances similar to that of pAza. The values for mmAbc in water and chloroform are 6.45 and 6.77 Å, respectively, whereas the value in the gas phase is 1.64 Å. This difference originates primarily in the *trans* form, which in water and chloroform has the highest standard deviation in span among the Abc amino acids and samples spans between 5 and 18 Å in conformers within 11.4 kJ/mol (i.e., a factor of 100 in stability at 25 °C) of the minimum. In the gas phase, *trans* mmAbc has clear preference for the more compact forms, likely reflective of favorable electrostatic interactions, leading to a sharp reduction in average span. For poAbc, the gating distance is consistently predicted as 6.7−7.0 Å across the three solvent models. The span-altering variable in this compound is rotation about the biaryl bonds. In the *trans* isomer, this rotation has little effect on span, and all observed spans were in the range 12.0−13.5 Å. In the *cis* isomer, rotation about the biaryl bonds can produce relatively long spans (up to 11.9 Å). However, these long conformers (span >10 Å) are disfavored by >30 kJ/mol in the gas phase and 15−20 kJ/mol in water, so they do not contribute significantly to the weighted average. The gating distance is thus well defined for poAbc in comparison to mmAbc, but it is little increased over pAza.

Isomers with Enhanced Gating Distances. Of all the isomers modeled, only two displayed gating distances substantially longer than that of pAza itself: pmAbc and mpAbc. The combination of *meta* and *para* linkages offers the optimum balance between flexibility and rigidity, and we thus examined the conformers in these two isomers more closely. All of the *trans* conformers for each are essentially isoenergetic (within 2 kJ/mol regardless of solvation model). For mpAbc, they fall into two groups, *syn* and *anti* (Figure 7), in which the torsional

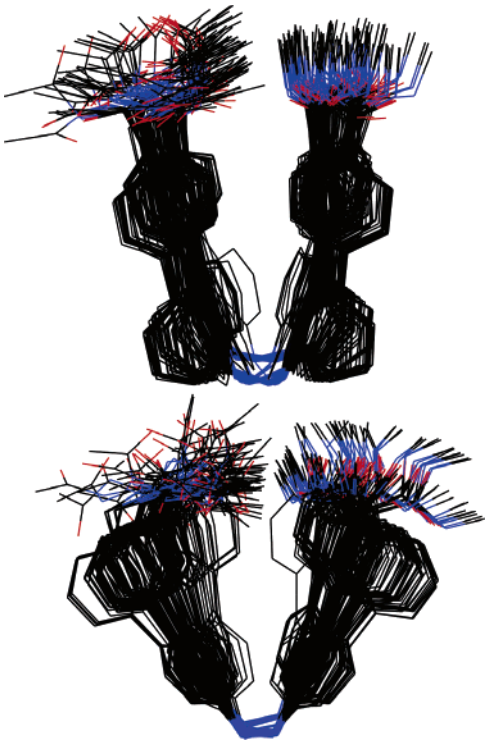

FIGURE 8. Superposed low-energy *cis* conformations of Ac-mpAbc-NHMe (top) and Ac-pmAbc-NHMe (bottom). Conformations within 11.4 kJ/mol of the minimum (water solvation model) were included (136 for mpAbc, 119 for pmAbc) and are oriented with the amino terminus on the upper left. Structures were superimposed on the basis of the carbons attached to the azo nitrogens and the carbons attached to the azobiphenyl nucleus (methylene and carbonyl). Color codes: black, carbon; blue, nitrogen; red, oxygen.

angle defined by the terminal substituents on the azobiphenyl is 0 ± 3° or 180 ± 1°, respectively. The *syn* conformers are 13.4 Å long, and the *anti* group includes about equal numbers of fully extended conformers (biaryl bonds *anti* to the azo linkage) that are 18.9 Å long and slightly retracted conformers (biaryl bonds *syn* to the azo linkage) that are 17.8 Å long. For pmAbc, the mix includes analogous *syn* (0 ± 4°) and *anti* (180 ± 2°) conformers, along with skewed forms of each (±77 ± 4° or ±104 ± 4°), as illustrated in Figure 7; all four forms have spans between 17.7 Å (*syn*) and 18.4 Å (*anti*).

The *cis* isomers cannot be subcategorized as cleanly and are best considered pictorially. Figure 8 shows a superposition of the low-energy conformers (within 11.4 kJ/mol of the minimum) for each compound. For preparation of this figure, conformations were taken from the simulation using water solvation because this set contained the greatest number of conformations overall, and energy differences between conformers tended to be muted, making for more inclusive sets. In mpAbc, the azobiphenyl nucleus displays a strong preference for a compact, folded form in which the termini are nearly parallel, and where the conformers are similar except for rotation of the substituent-arene bonds and the benzylic C−N bond. The main consequence of *para* substitution on the inner rings in pmAbc is to displace the outer rings from one another; this displacement tends to increase span while also giving the *meta*-substituted outer rings more conformational freedom about the biaryl linkage, thereby increasing heterogeneity in span. These effects are most apparent in the water calculation, where the span $R \pm s_R$ is 5.79 ± 1.35 Å for mpAbc versus 6.67 ± 2.21 Å for pmAbc. In the chloroform and gas-phase simulations, the greater conformational freedom of pmAbc is damped by electrostatic effects, which favor the more compact forms, reducing both span and standard deviation in span.

Both mpAbc and pmAbc are predicted to have significantly improved distance-gating performance over pAza. Assessment of which of the two azobiphenyl-based amino acids is superior depends on the purpose to which the amino acid is to be put along with subjective considerations. The main drawback to mpAbc is the conformational heterogeneity in its *trans* configuration, with the isoenergetic *syn* and *anti* conformers having substantially different spans. In contrast, the main drawback to pmAbc is the greater average span and greater conformational heterogeneity in its *cis* form. If average gating distance is the dominant criterion, then pmAbc has a slight advantage according to the calculations (gating distance of 11.4 vs 9.9 Å in water). If, however, maximal gating distance is dominant (i.e., the span of *trans* mpAbc is taken as that of the longer *anti* conformers rather than the *syn*/*anti* average), then mpAbc has a slight advantage due to its more compact and uniform *cis* form (ΔR of 12.5 Å for mpAbc versus 11.4 Å for pmAbc in water). It is helpful to consider these values in terms of peptide units. The spans in the *cis* conformations of mp- and pmAbc are very similar to the 5 Å span ($C_{\alpha i} \rightarrow C_{i+1}$) of a conventional dipeptide, whereas the spans of the *trans* conformations are very similar to the 18 Å span of a fully extended pentapeptide. Thus, the photochemical contraction in mp- or pmAbc is equivalent to the removal of three amino acids from the backbone.

For the initial application of Abc amino acids, generation of a light-regulated nuclear localization signal (NLS) peptide,[30] we favored the latter criterion and therefore made mpAbc the primary focus of our synthetic efforts. We were also guided in this direction by the heterogeneity of *cis* forms in pmAbc and the judgment that the girth of *cis* pmAbc might be disadvantageous for our applications, as it would be more intrusive than the svelter mpAbc in a polypeptide.

Synthesis of Selected Abc Amino Acids in Protected Form. Having identified mpAbc as the prime candidate for our peptide engineering applications, we sought a synthesis that would deliver ample quantities of its *N*-Fmoc derivative for use in solid-phase peptide synthesis. A route was planned in which the key reactions were a nitroso-aniline condensation to form the azo linkage and Suzuki couplings[45] to form the biaryl units (Scheme 1). During preliminary studies, we encountered difficulty in preparing and purifying arylnitroso compounds containing Fmoc-protected amines. Therefore, the biaryls were constructed to give an N-terminal anilino component and a C-terminal nitroso component for condensation to the azobenzene.

With this strategy, the target could be prepared convergently from four simple building blocks: *m*-nitro and *m*-aminophenylboronic acids, which are commercially available, along with *p*-iodobenzoic acid *tert*-butyl ester and *N*-Fmoc-protected *p*-iodobenzylamine, both of which are readily derived from commercial materials by installation of the protecting groups. The modular nature of the route made it amenable to the production of other Abc isomers. To test its generality and to provide important controls for peptide engineering efforts, we also targeted moAbc and mmAbc. These share the same boronic acid building blocks and employ different halide components,

(45) (a) Suzuki, A. *Pure Appl. Chem.* **1985**, *57*, 1749−1758. (b) Suzuki, A.; Miyaura, N. *Chem. Rev.* **1995**, *95*, 2457−2483.

SCHEME 1. Synthesis of Fmoc-mxAbc-O*t*-Bu Isomers 13a−c

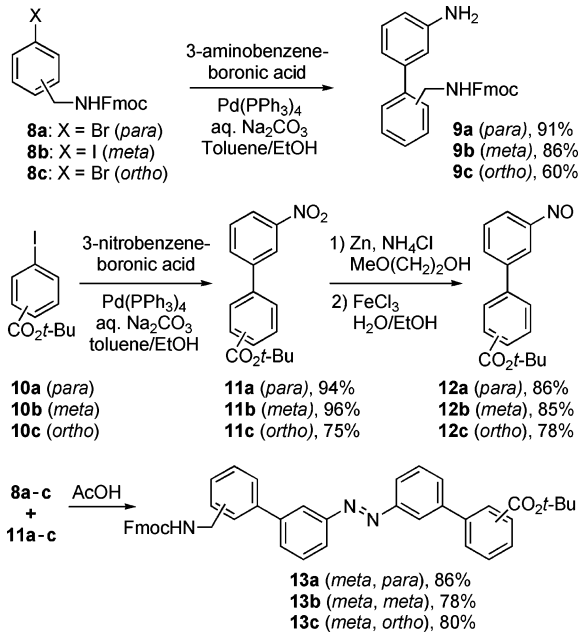

SCHEME 2. Synthesis of Fmoc-ppAbc-O*t*-Bu 13d

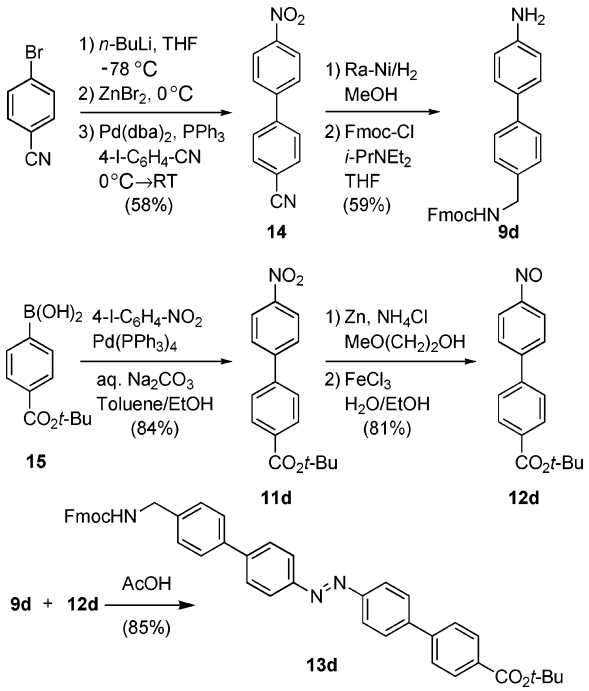

all of which are readily available. Finally, we targeted ppAbc as the parent of the Abc family and most direct higher homologue of pAza. For this compound, a variation of the approach was employed in which the amino-terminal biphenyl unit was prepared via a Negishi coupling,[46] and the carboxy-terminal biphenyl unit was prepared via a Suzuki coupling in which the outer ring entered as a boronic acid rather than a halide.

Syntheses of the three protected Fmoc-mxAbc-O*t*-Bu isomers proceeded smoothly as planned. The first requirement in all cases was protection of the terminal substituents. All three isomers of iodobenzoic acid were converted cleanly to their *tert*-butyl esters **10a**−**c** by sulfuric acid catalyzed reaction with isobutylene in dichloromethane. Likewise, Fmoc protected halobenzylamines **8a**−**c** were prepared by reaction of the corresponding amines with Fmoc-Cl in 80−84% yield. Suzuki couplings of the latter to *m*-aminophenylboronic acid yielded the Fmoc-protected N-terminal biphenyl components **9a**−**c**, in good yield for the *meta*- and *para*-substituted halides but in modest yield (60%) for the *ortho*-substituted halide. Coupling of the three *tert*-butyl iodobenzoates to *m*-nitrophenylboronic acid under the same conditions yielded nitro-functionalized, *tert*-butyl-protected C-terminal biphenyl components **11a**−**c**, with comparable yields for the *meta*- and *para*-halides and improved yield for the *ortho* halide. The nitroso fragments **12a**−**c** were prepared by reduction of nitro compounds **11a**−**c** to hydroxylamines with zinc and ammonium chloride in 2-methoxyethanol, followed by in situ reoxidation to nitroso compounds with ferric chloride in water/ethanol. Finally, N-terminal aniline components **9a**−**c** and corresponding C-terminal nitroso components **12a**−**c** were condensed in acetic acid for 24 h at room temperature to afford protected Abc derivatives **13a**−**c**, which were obtained in 78−86% yield after purification by flash column chromatography.

The synthesis of Fmoc-ppAbc-O*t*-Bu **13d** involved a variant of the basic approach in which the N-terminal biphenyl component was prepared via a Negishi coupling and the C-terminal biphenyl component was prepared via a Suzuki coupling where the outer ring entered as a boronic acid rather than a halide (Scheme 2). Thus, 4-bromobenzonitrile was lithiated with *n*-BuLi in THF at −78 °C, transmetalated with $ZnBr_2$, and then coupled to 4-iodonitrobenzene in the presence of catalytic $Pd(dba)_2/PPh_3$ to afford 4-cyano-4′nitrobiphenyl **14** in 58% yield. Reduction of this compound with Raney nickel in methanol under 50 psi of H_2 overnight, followed by selective Fmoc protection of the benzylic amine with Fmoc-Cl, yielded N-terminal biphenyl component **9d** in 59% for the two steps. The relatively low isolated yields from these reactions owe significantly to the difficulty of purifying the poorly soluble biphenyl derivatives. C-Terminal biphenyl component **11d** was prepared by Suzuki coupling of 4-(*t*-butoxycarbonyl)phenylboronic acid **15** with 4-iodonitrobenzene. The remaining steps were conducted as for the mxAbc isomers, with reduction of **11d** to the corresponding nitroso compound **12d** proceeding in 81% yield and condensation with N-terminal component **9d** proceeding in 85% yield to afford Fmoc-ppAbc-O*t*-Bu **13d**.

Peptide Synthesis with mpAbc. To test the chemical and photochemical properties of mpAbc, we synthesized a model peptide, STPPK(mpAbc)KKRKV, in which mpAbc was inserted into the middle of the NLS of the SV40 large T antigen.[47] This peptide was chosen because of intended applications for mpAbc in the nuclear import field and because of the peptide's high water solubility, which would allow us to examine chemical and photochemical behavior in aqueous buffer. Removal of the *tert*-butyl ester from Fmoc-mpAbc-O*t*-Bu **13a** with 95% TFA/5% H_2O proceeded uneventfully and afforded Fmoc-mpAbc-OH in 85% yield. The mpAbc-containing peptide was synthesized manually using standard solid-phase Fmoc procedures employing PyBOP[48] as the coupling agent. Couplings with

(46) Negishi, E. *J. Am. Chem. Soc.* **1982**, *82*, 340−348.

(47) (a) Lanford, R. E.; Butel, J. S. *Cell* **1984**, *37*, 801−813. (b) Kalderon, D.; Richardson, W. D.; Markham, A. F.; Smith, A. E. *Nature (London, U. K.)* **1984**, *311*, 33−38. (c) Kalderon, D.; Roberts, B. L.; Richardson, W. D.; Smith, A. E. *Cell* **1984**, *39*, 499−509.

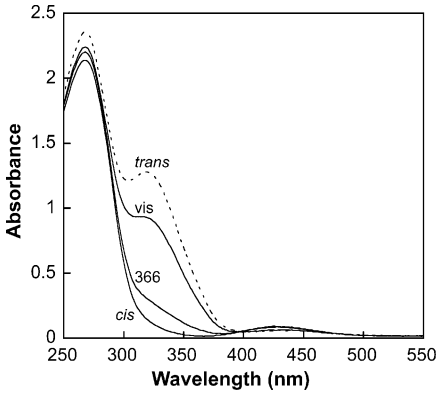

FIGURE 9. UV spectra of the soluble peptide STPPK(mpAbc)-KKRKV. Spectra for *cis* and *trans* isomers were recorded from isolated HPLC fractions of the pure isomers (in water containing ca. 25% v/v acetonitrile and 0.1% v/v CF_3CO_2H). Photostationary states were produced by irradiation of the *cis* sample in the cuvette with monochromatic 366-nm light (labeled 366) or polychromatic white light from a halogen lamp (labeled vis). The spectrum of the *trans* isomer is shown in dashed line to emphasize that it was obtained from a different sample and was scaled to correspond to the same concentration as for the other three spectra on the basis of superimposition of derived 366-nm and white light photostationary state spectra.

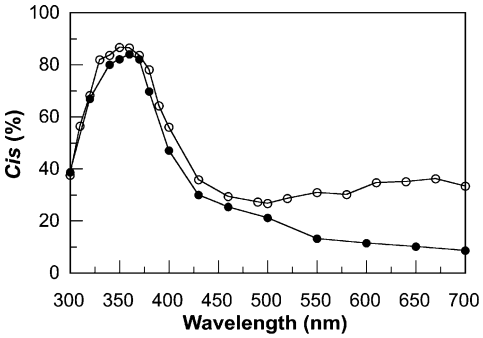

FIGURE 10. Isomeric composition of the model peptide STPPK-(mpAbc)KKRKV as a function of wavelength. Filled circles show the results of a decreasing wavelength scan (700−300 nm) starting from the *trans* isomer. Open circles show the results of an increasing wavelength scan (300−700 nm). The divergence of the results above 500 nm indicates failure to reach the photostationary state due to a vanishing extinction coefficient.

standard amino acids employed 2.0 equiv of Fmoc-amino acid and a 2-h reaction time. For mpAbc, it was desirable to conserve the protected amino acid, so 1.5 equiv was used, and the reaction time was increased to 3 h.

Coupling at each step of the synthesis was judged to be qualitatively complete using the Kaiser ninhydrin test[49] (or the chloranil test[50] for proline). This qualitative observation was borne out by quantitative Fmoc analysis of the couplings involving mpAbc, which showed coupling efficiencies of 99% at the N- and C-terminal ends of mpAbc, with an estimated uncertainty of ±3%. The completed peptide was cleaved and deprotected in conventional fashion (95% TFA/5% H_2O, 2 h) and purified by RP-HPLC. This example demonstrated that mpAbc can be incorporated into synthetic peptides with high efficiency and with no impact on downstream procedures (coupling, deprotection, and cleavage) using conventional Fmoc methods. Subsequent incorporation of mpAbc into a large number of peptides has proceeded uneventfully. The only incompatibility we have noted is the apparent decomposition of mpAbc when trialkylsilanes are included in the TFA deprotection/cleavage procedure. For situations where a more powerful scavenger than water was required, we have successfully employed 1,2-ethanedithiol.

Photochemical Properties of mpAbc. In order for mpAbc to be useful for applications, it had to maintain the photochemical properties of azobenzene. These were examined in the context of the synthesized model peptide using UV−vis spectroscopy and HPLC. The photoisomers of the peptide were readily separable by HPLC and could be asssigned as *cis* and *trans* on the basis of their absorbance spectra and complete thermal equilibration to the *trans* form. Both isomers displayed characteristic, azobenzene-like absorbance spectra (Figure 9). In the pure *trans* form, absorption maxima were observed at 268, 319, and 429 nm. In the pure *cis* form, the 268-nm peak was slightly less intense, the 319-nm peak was absent, and the weak 429-nm peak had shifted to 425 nm and become approximately 50% more intense. Irradiation with handheld UV or white light sources for several minutes led to corresponding photostationary states displaying well-resolved intermediate spectra.

We next sought to determine the photostationary state isomer composition as a function of wavelength (Figure 10). As the *cis* and *trans* photoisomers of the peptide were fully resolved by RP-HPLC, we relied on peak area integrals from chromatograms run with UV detection at 290 nm, which is an essentially isosbestic wavelength and therefore gives peak areas proportional to concentration. A quartz cuvette containing a solution of the peptide in phosphate buffered saline (pH 7.4) was placed in the sample holder of an SLM-Aminco 8000 fluorescence spectrometer and irradiated with a series of increasing wavelengths from 300 to 700 nm. An analogous experiment in which irradiation started at the longer wavelength and progressed to the shorter one was run starting with a dark-adapted (>98% *trans*) sample of the peptide. The results of the two experiments were in excellent agreement over the range 300−500 nm, confirming that the isomer composition in that range accurately reflects the photostationary state; moreover, the intermediate UV−vis spectra shown in Figure 9 are fully consistent with the isomer compositions found by HPLC. At wavelengths above 500 nm, the data diverge, indicating that the photostationary state could not be reached in the 20-min irradiation period because of the low extinction coefficient of the chromophore and the modest light intensity available. Optimal conversion to *cis* (about 85%) was achieved with 360-nm light, near an absorbance minimum for *cis* isomer. The greatest *trans* population in a photostationary state (about 75%) was achieved with 500 nm light.

Finally, we examined the thermal *cis* → *trans* isomerization of the peptide in PBS at pH 7.4. For this set of experiments, samples of the peptide in a quartz cuvette were irradiated with 366 nm light to produce the *cis*-rich PSS, and recovery of the absorbance at 320 nm was monitored over time at several temperatures (Figure 11). During the recovery period, samples were kept in the spectrometer sample compartment, out of the light beam except for periodic 0.25-s absorbance measurements and under constant electronic temperature control. At 37 °C, no recovery could be detected over the course of 12 h. At higher temperatures, clean first-order recovery was observed, with half-lives of 16 h at 60 °C and 100 min at 80 °C.

(48) Coste, J.; Le-Nguyen, D.; Castro, B. *Tetrahedron Lett.* **1990**, *31*, 205−208.
(49) Kaiser, E.; Colescott, R. L.; Bossinger, C. D.; Cook, P. I. *Anal. Biochem.* **1970**, *34*, 595−598.
(50) Christensen, T. *Acta Chem. Scand., Ser. B* **1979**, *B33*, 763−766.

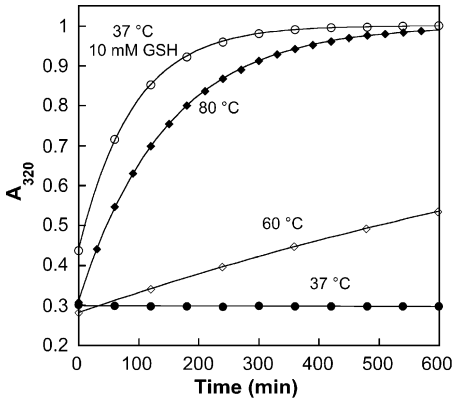

FIGURE 11. Thermal *cis* → *trans* isomerization of the model peptide STPPK(mp-Abc)KKRKV in phosphate-buffered saline at pH 7.4. Samples were irradiated with 366-nm light and then allowed to recover in the dark at the indicated temperatures (stoppered at 37 °C or overlaid with mineral oil at 60 and 80 °C to prevent evaporation). Markers show experimental measurements, and lines show computationally modeled, best-fit progress curves (linear for 37 °C without GSH, first-order for others): (●) 37 °C; (○) 37 °C with 10 mM GSH; (◊) 60 °C; (♦) 80 °C. To facilitate comparison, data were scaled to a common final absorbance of 1.0 (actual 0.87−0.95).

An important consideration for prospective applications of mpAbc in vivo was its stability to glutathione (γ-Glu-Cys-Gly, abbreviated GSH), an abundant intracellular thiol. Although we did not observe any degradation of the peptide, even upon extended incubation with 10 mM GSH (near the upper end of concentrations that might be encountered in mammalian cells[51]), we did observe that GSH strongly catalyzed *cis* → *trans* isomerization. Thus, although the rate of recovery at 37 °C without GSH was negligible, recovery at the same temperature in the presence of 10 mM GSH was rapid, following clean pseudo-first-order kinetics with a half-life of 60 min (faster than the uncatalyzed reaction at 80 °C). Although the mechanism of catalysis is unknown, one possibility is that a GSH-derived thiol radical or thiolate anion adds reversibly to the N═N double bond, transiently reducing bond order and freeing rotation. In our experience, the accelerated relaxation has proven very useful in fully dark-adapting substrates, a process that otherwise requires temperatures incompatible with sensitive biomaterials or impractically long reaction times. If the PSS composition must be held constant for an extended period of time, continuous irradiation or periodic touch-up irradiation can be used to maintain it.

Conclusions

A desire for photoelastic amino acids with enhanced distance gating provided the impetus for a molecular modeling study to evaluate options for amplifying the distance gating of the known azobenzene-based amino acid pAza by replacing the azobenzene nucleus with an azobiphenyl nucleus. This study revealed that distance gating varied strongly with substitution pattern and focused attention on a particular isomer, mpAbc, with significantly enhanced distance gating. An efficient, convergent, and modular synthesis of Fmoc-mpAbc-OH was designed to prepare the target amino acid in quantity and in a form suitable for use in solid-phase peptide synthesis. The synthesis proceeded in approximately 50% overall yield from simple building blocks, and its versatility was demonstrated by application to three other Abc isomers. mpAbc was efficiently incorporated into a synthetic model peptide and displayed the characteristic spectral and photochemical properties of azobenzenes, with maximal conversion to the *cis* form (85%) occurring upon irradiation with 360 nm light. Dark isomerization of the model peptide was negligible over the course of 10 h in aqueous buffer at physiological pH and temperature but was appreciably catalyzed by GSH ($t_{1/2}$ = 60 min at 37 °C in the presence of 10 mM GSH at pH 7.4). These properties, along with the predicted conformational properties, make mpAbc suitable for applications in peptide engineering.

Experimental Section

Carbamic Acid, [4-Bromophenyl]methyl-9*H*-fluoren-9-ylmethyl Ester (*N*-Fmoc-4-bromobenzylamine) (8a). To a mixture of 4-bromobenzylamine hydrochloride (1.0 g, 4.5 mmol) and diisopropylethylamine (1.80 mL, 10.4 mmol) in anhydrous THF (20 mL) at 0 °C was added dropwise over 10 min a solution of Fmoc-Cl (1.16 g, 4.5 mmol) in 5 mL of anhydrous THF. The reaction mixture was slowly warmed to room temperature, stirred overnight, and diluted with 50 mL of EtOAc and 10 mL of water. The organic layer was separated, washed with brine, and dried over $MgSO_4$. The solvent was removed under reduced pressure, and the residue was purified by recrystallization from $CHCl_3$/hexanes giving **8a** (1.54 g, 84%) as a white solid: mp 150−151 °C; TLC R_f = 0.38 (hexanes/EtOAc, 3:1); IR (KBr) 3327, 2373, 1694, 1267 cm^{-1}; ^1H NMR (200 MHz, $CDCl_3$) δ 4.21 (t, 1H, J = 6.7 Hz), 4.31 (d, 2H, J = 6.3 Hz), 4.48 (d, 2H, J = 6.7 Hz), 5.08 (br t, 1H), 7.10 (d, 2H, J = 8.2 Hz), 7.29−7.45 (m, 6H), 7.58 (d, 2H, J = 7.3 Hz), 7.76 (d, 2H, J = 7.2 Hz); ^{13}C NMR (50 MHz, $CDCl_3$) δ 44.4, 47.3, 66.7, 119.9, 121.5, 124.9, 127.0, 127.7, 129.1, 131.7, 137.4, 141.3, 143.8, 156.4; HRMS−FAB (M + Na^+) calcd for $C_{22}H_{18}BrNNaO_2$ 430.04187 and 432.03991, found 430.04118 and 432.04010.

Carbamic Acid, [3-Iodophenyl]methyl-9*H*-fluoren-9-ylmethyl Ester (8b). Fmoc protection of 3-iodobenzylamine (1.0 g, 4.3 mmol) with Fmoc-Cl (1.11 g, 4.3 mmol) and DIPEA (0.9 mL, 5.2 mmol) was performed as described for **8a** to afford 1.63 g of **8b** (83%) as a white solid after recrystallization from $CHCl_3$/hexanes: mp 159 °C; TLC R_f = 0.40 (hexanes/EtOAc, 3:1); IR (KBr) 3313, 1691, 1540, 1254, 741 cm^{-1}; ^1H NMR (200 MHz, $CDCl_3$) δ 4.22 (t, 1H, J = 7.4 Hz), 4.32 (d, 2H, J = 6.2 Hz), 4.46 (d, 2H, J = 6.7 Hz), 5.20 (br t, 1H), 7.05 (t, 1H, J = 7.8 Hz), 7.25−7.43 (m, 5H), 7.57−7.62 (m, 4H), 7.76 (d, 2H, J = 7.2 Hz); ^{13}C NMR (50 MHz, $CDCl_3$) δ 44.3, 47.2, 66.8, 94.6, 120.0, 124.9, 126.7, 127.1, 127.7, 130.4, 136.4, 136.6, 140.8, 141.3, 143.8. 156.4; HRMS−FAB (M + Na^+) calcd for $C_{22}H_{18}INNaO_2$ 478.0280, found 478.02755.

Carbamic Acid, [2-Bromophenyl]methyl-9*H*-fluoren-9-ylmethyl Ester (8c). Fmoc protection of 2-bromobenzylamine (1.0 g, 4.5 mmol) with Fmoc-Cl (1.16 g, 4.5 mmol) and DIPEA (0.9 mL, 5.4 mmol) was performed as described for **8a** to afford 1.47 g (80%) of **8c** as a white solid after recrystallization from $CHCl_3$/hexanes: mp 155−156 °C; TLC R_f = 0.49 (hexanes/EtOAc, 3:1); IR (KBr) 3310, 3060, 2939, 2360, 1694, 1537, 1286, 741 cm^{-1}; ^1H NMR (200 MHz, $CDCl_3$) δ 4.21 (t, 1H, J = 6.7 Hz), 4.43 (d, 4H, J = 6.9 Hz), 5.27 (br t, 1H), 7.15 (td, 1H, J = 7.5, 1.8 Hz), 7.29−7.43 (m, 5H), 7.60 (t, 4H, J = 6.7 Hz), 7.76 (d, 2H, J = 7.1 Hz); ^{13}C NMR (50 MHz, $CDCl_3$) δ 45.4, 47.3, 66.8, 119.9, 123.6, 124.9, 125.0, 127.0, 127.6, 129.2, 130.0, 132.8, 137.4, 141.3, 143.9, 156.3; HRMS−FAB (M + Na^+) calcd for $C_{22}H_{18}BrNNaO_2$ 430.04187 and 432.03991, found 430.04260 and 432.04067.

Carbamic Acid, [(3′-Amino[1,1′-biphenyl]-4-yl)methyl]-9*H*-fluoren-9-ylmethyl Ester (9a). A solution of *N*-Fmoc-4-bromobenzylamine **8a** (2.0 g, 4.9 mmol), 3-aminobenzeneboronic acid (805 mg, 5.9 mmol), tetrakis(triphenylphosphine)palladium(0) (170

(51) DeLeve, L. D.; Kaplowitz, N. *Pharmacol. Ther.* **1991**, *52*, 287−305.

mg, 3 mol %), and 5 mL of 2 M aqueous Na_2CO_3 in toluene (150 mL) and ethanol (10 mL) was refluxed and stirred for 12 h. The reaction mixture was cooled to room temperature and diluted with EtOAc (300 mL) and dd H_2O (100 mL). The organic layer was washed with brine and dried over $MgSO_4$, the solvent was removed under reduced pressure, and the residue was purified by recrystallization from $CHCl_3$/hexanes to afford 2.23 g (91%) of **9a** as a white solid: mp = 142−143 °C; TLC R_f = 0.23 (hexanes/EtOAc, 3:2); IR (KBr) 3370, 3008, 2984, 1701, 1531, 1349, 1304, 1160, 1122, 777 cm^{-1}; ^1H NMR (300 MHz, DMSO-d_6) δ 4.21 (d, 2H, J = 6.0 Hz), 4.24 (t, 1H, J = 6.4 Hz), 4.37 (d, 2H, J = 7.2 Hz) 5.16 (br s, 2H), 6.55 (d, 1H, J = 7.2 Hz), 6.76 (d, 1H, J = 6.9 Hz), 6.82 (br s, 1H), 7.09 (t, 1H, J = 7.8 Hz), 7.27 (d, 2H, J = 8.1 Hz), 7.33 (t, 2H, J = 7.5 Hz), 7.43 (t, 2H, J = 7.3 Hz), 7.49 (d, 2H, J = 8.1 Hz), 7.71 (d, 2H, J = 7.5 Hz), 7.84−7.92 (m, 1H), 7.90 (d, 2H, J = 7.8 Hz); ^{13}C NMR (75 MHz, DMSO-d_6) δ 43.5, 46.8, 65.3, 112.0, 113.0, 114.3, 120.12, 125.2, 126.3, 127.0, 127.5, 127.6, 129.4, 138.6, 139.6, 140.7, 140.8, 143.9, 149.1, 156.4; HRMS−FAB (M + Na^+) calcd for $C_{28}H_{24}N_2NaO_2$ 443.1736, found 443.17304.

Carbamic Acid, [(3′-Amino[1,1′-biphenyl]-3-yl)methyl]-9*H*-fluoren-9-ylmethyl Ester (9b). The Suzuki coupling procedure was the same as described for **9a**. From 900 mg (2.0 mmol) of **8b** and 360 mg (2.6 mmol) of 3-aminobenzeneboronic acid was obtained 720 mg (86%) of **9b** as a white solid. The crude product was purified by flash column chromatography (hexanes/EtOAc, 3:2): mp 139−140 °C; TLC R_f = 0.24 (hexanes/EtOAc, 2:1); IR (KBr) 3453, 3367, 3317, 3063, 3038, 3018, 2950, 2920, 2363, 1692, 1541, 1256 cm^{-1}; ^1H NMR (200 MHz, $CDCl_3$) δ 3.56 (br s, exchanges with D_2O, 2H), 4.23 (t, 1H, J = 6.8 Hz), 4.37−4.50 (m, 4H), 5.20 (br t, 1H), 6.68 (ddd, 1H, J = 7.9, 2.3, 1.0 Hz), 6.87 (t, 1H J = 1.9 Hz), 6.97 (ddd, 1H, J = 6.6, 2.6, 1.0 Hz), 7.17−7.42 (m, 7H), 7.46 (t, 2H, J = 6.3 Hz), 7.60 (d, 2H, J = 7.0 Hz), 7.76 (d, 2H, J = 7.4 Hz); ^{13}C NMR (50 MHz, $CDCl_3$) δ 45.2, 47.3, 66.7, 113.9, 114.3, 117.8, 119.9, 125.0, 126.3, 126.9, 127.0, 127.7, 129.0, 129.7, 138.8, 141.3, 141.9, 142.0, 143.9, 146.7, 156.5; HRMS−FAB (M + Na^+) calcd for $C_{28}H_{24}N_2NaO_2$ 443.17355, found 443.1737.

Carbamic Acid, [(3′-Amino[1,1′-biphenyl]-2-yl)methyl]-9*H*-fluoren-9-ylmethyl Ester (9c). The Suzuki coupling procedure was the same as described for **9a**. From 820 mg (2.0 mmol) of **8c** and 360 mg (2.6 mmol) of 3-aminobenzeneboronic acid was obtained 500 mg (60%) of **9c** as a white solid. The crude product was purified by flash column chromatography: mp 135−136 °C; TLC R_f = 0.23 (hexanes/EtOAc, 3:2); IR (KBr) 3327, 3042, 2934, 1694, 1534, 1267, 1145, 742 cm^{-1}; ^1H NMR (200 MHz, $CDCl_3$) δ 3.69 (br s, exchanges with D_2O, 2H), 4.18 (t, 1H, J = 6.7 Hz), 4.33−4.39 (m, 4H), 4.84 (br s, 1H), 6.58−6.60 (m, 1H), 6.66 (dt, 2H, J = 7.9, 1.7 Hz), 7.15−7.43 (m, 9H), 7.55 (d, 2H, J = 7.3 Hz), 7.75 (d, 2H, J = 7.2 Hz); ^{13}C NMR (50 MHz, $CDCl_3$) δ 42.9, 47.3, 66.6, 113.9, 115.6, 119.3, 119.9, 125.1, 127.1, 127.3, 127.7, 128.3, 129.3, 129.9, 135.7, 141.3, 141.8, 143.9, 146.4, 156.3; HRMS−FAB (M + Na^+) calcd for $C_{28}H_{24}N_2NaO_2$ 443.17355, found 443.17232.

4′-Nitro-1,1′-biphenyl-4-carbonitrile (14). To a solution of 4-bromobenzonitrile (1.82 g, 10.0 mmol) in 10 mL of anhydrous THF at −78 °C was added over 5 min *n*-BuLi (4 mL, 10 mmol, 2.5 M in hexanes), leading to the formation of a reddish-brown precipitate. After 30 min with stirring at −78 °C, a solution of $ZnBr_2$ in 10 mL of anhydrous THF was slowly added to the reaction mixture, which was warmed to 0 °C for 5 min and then cooled back to −20 °C. Bis(dibenzylideneacetone) palladium(0) (280 mg, 5 mol %), triphenylphosphine (520 mg, 20 mol %) and 4-iodonitrobenzene (2.0 g, 8.0 mmol) in 20 mL of anhydrous THF were added to the reaction mixture, which was allowed to warm to room temperature and was stirred overnight. After dilution with EtOAc (100 mL), the reaction mixture was washed successively with water and brine. The organic layer was dried over $MgSO_4$, the solvent was removed under reduced pressure, and the product was purified by recrystallization from THF to afford 700 mg (58%) of **14** as a pale yellow solid: mp 180−181 °C; TLC R_f = 0.25 (hexanes/EtOAc, 4:1); IR (KBr) 3096, 2925, 2227, 1602, 1512, 1348 cm^{-1}; ^1H NMR (200 MHz, $CDCl_3$) δ 7.70−7.81 (m, 6H), 8.33 (dt, 2H, J = 9.0, 2.1 Hz); ^{13}C NMR (50 MHz, $CDCl_3$) δ 112.6, 118.3, 124.3, 128.06, 128.12, 132.9, 143.1, 145.3, 147.8. The ^1H NMR data are in accord with those previously reported by Lan et al.[52] but there are discrepancies in the ^{13}C NMR data, which were reported as follows ($CDCl_3$, 75.4 MHz) δ 118.6, 124.5, 124.6, 128.2, 128.3, 128.4, 133.2, 143.4, 145.6. Chemical shifts calculated from the reference spectrum[53] of 4-nitrobiphenyl in $CDCl_3$ and chemical shift increments for cyano,[54] assuming effects only on the cyano-bearing ring, are as follows (assignment and calculated minus our observed values in parentheses): 113.16 (0.56, C4), 123.95 (−0.36, C3′), 127.62 (−0.44, C2′), 127.96 (−0.16, C2), 132.65 (−0.21, C3), 142.87 (−0.20, C1), 146.92 (1.58, C4′), 147.41 (−0.43, C1′). The close correspondence of the calculated values with our observed values allows us to assign the peak at δ 118.3 as the nitrile carbon and indicates that in the literature values, two resonances of quaternary carbons are missing (112.6 and 147.8) and two of the reported peaks are artifactual or non-compound related (124.5 or 124.6 and 128.2 or 128.3 or 128.4).

Carbamic Acid, [(4′-Amino[1,1′-biphenyl]-4-yl)methyl]-9*H*-fluoren-9-ylmethyl Ester (9d). 4-Cyano-4′-nitrobiphenyl **14** (1.12 g, 5.0 mmol) and Raney Ni (100 mg) in 50 mL of methanol were shaken under 50 psi of H_2 overnight. The reaction mixture was filtered through Celite, washed through with 50 mL of EtOAc, and extracted into 1 M HCl (2 × 50 mL). The combined acid layer was neutralized with 3 M NaOH and extracted with benzene (2 × 50 mL). After removal of the solvent by rotary evaporation, the crude diamine was dissolved in 50 mL of anhydrous THF, and Fmoc-Cl (1.0 g, 4.0 mmol) in 5 mL of anhydrous THF was added dropwise over 10 min at 0 °C. The reaction mixture was allowed to warm to room temperature and was stirred overnight before being diluted with 100 mL of EtOAc and 40 mL of dd H_2O. The organic layer was washed with brine and dried over $MgSO_4$, the solvent was removed under reduced pressure, and the residue was purified by flash chromatography (3:2 hexanes/EtOAc with 1% triethylamine) to afford 1.23 g (59%) of **9d** as a pale yellow solid: mp 167−169 °C; TLC R_f = 0.50 (hexanes/EtOAc, 1:1); IR (KBr) 3367, 3325, 3038, 1671, 1541, 1256 cm^{-1}; ^1H NMR (200 MHz, acetone-d_6) δ 4.25 (t, 1H, J = 7.6 Hz), 4.30−4.45 (m, 4H), 4.75 (br s, exchanges with D_2O, 2H), 6.74 (d, 2H, J = 7.2 Hz), 6.98 (br s, 1H), 7.23−7.42 (m, 8 H), 7.47 (d, 2H, J = 8.6 Hz), 7.70 (d, 2H, J = 8.3 Hz), 7.85 (d, 2H, J = 8.2 Hz); ^{13}C NMR (50 MHz, acetone-d_6) δ 44.7, 47.9, 66.6, 115.3, 120.5, 125.9, 126.4, 127.7, 128.0, 128.2, 128.4, 129.6, 137.9, 140.8, 141.9, 144.9, 148.7, 157.1; HRMS−FAB (M + Na^+) calcd for $C_{28}H_{24}N_2NaO_2$ 443.17355, found 443.17401.

Iodobenzoic Acid *tert*-Butyl Esters (10a−c). Representative Procedure. Into a cooled (dry ice−acetone) slurry of 2-iodobenzoic acid (5.0 g, 20 mmol) and concentrated H_2SO_4 (0.3 mL) in CH_2Cl_2 (50 mL) in a pressure tube was slowly poured liquid isobutylene (30 mL, excess), which had been precondensed in a cold trap filled with dry ice−acetone. The pressure tube was sealed, and the reaction mixture was stirred at room temperature behind a safety shield until it became clear (2 d), at which point the reaction was cooled to −78 °C and the cap of the pressure tube was removed. The reaction mixture was allowed to warm with stirring to room temperature, quenched with 100 mL of saturated aqueous $NaHCO_3$, and extracted into EtOAc (50 mL). After washing with water and brine, the organic layer was dried over $MgSO_4$ and concentrated under reduced pressure. Purification of the crude product by flash column chromatography on silica with 50:1 hexanes/EtOAc as the eluent afforded 2-iodobenzoic acid *tert*-butyl ester **10c** in 84% yield

(52) Lan, P.; Berta, D.; Porco, J. A., Jr.; South, M. S.; Parlow, J. J. *J. Org. Chem.* **2003**, *68*, 9678−9686.

(53) Bailey, W. F.; Cioffi, E. A. *Magn. Reson. Chem.* **1987**, *25*, 181−183.

(54) Pretsch, E.; Furst, A.; Robien, W. *Anal. Chim. Acta* **1991**, *248*, 415−428.

as a pale yellow oil: TLC R_f = 0.73 (hexanes/EtOAc, 5:1); ^{1}H NMR (200 MHz, $CDCl_3$) δ 1.60 (s, 9H), 7.09 (td, 1H, J = 7.9, 1.8 Hz), 7.36 (td, 1H, J = 7.8, 1.3 Hz), 7.67 (dd, 1H, J = 7.9, 1.8 Hz), 7.93 (dd, 1H, J = 7.8, 1.3 Hz); ^{13}C NMR (50 MHz, $CDCl_3$) δ 28.1, 81.6, 93.4, 127.8, 130.4, 131.9, 137.4, 140.9, 166.2.

4-Iodobenzoic Acid *tert*-Butyl Ester (10a). TLC R_f = 0.54 (hexanes/EtOAc, 25:1); ^{1}H NMR (200 MHz, $CDCl_3$) δ 1.58 (s, 9H), 7.67 (d, 2H, J = 8.8 Hz), 7.76 (d 2H, J = 8.8 Hz); ^{13}C NMR (50 MHz, $CDCl_3$) δ 28.1, 81.4, 100.0, 131.5, 137.5, 165.2.

3-Iodobenzoic Acid *tert*-Butyl Ester (10b). TLC R_f = 0.43 (hexanes/EtOAc, 25:1); ^{1}H NMR (200 MHz, $CDCl_3$) δ 1.58 (s, 9H), 7.13 (t, 1H, J = 7.9 Hz), 7.82 (dt, 1H, J = 7.9, 1.3 Hz), 7.92 (dt, 1H, J = 7.8, 1.3 Hz), 8.28 (t, 1H, J = 1.4 Hz); ^{13}C NMR (50 MHz, $CDCl_3$) δ 28.1, 81.6, 93.7, 128.6, 129.8, 133.9, 138.3, 141.2, 164.1.

4-Carboxybenzeneboronic Acid *tert*-Butyl Ester (15). To a cooled (dry ice−acetone) slurry of 4-carboxybenzeneboronic acid (2.0 g, 12 mmol) and concentrated H_2SO_4 (0.5 mL) in CH_2Cl_2 (20 mL) in a pressure tube was slowly poured liquid isobutylene (40 mL, excess), which had been precondensed on a coldfinger containing dry ice−acetone. The pressure tube was sealed, and the reaction mixture was stirred at room temperature for 24 h until it became clear, at which point the reaction mixture was cooled to −78 °C and the cap of pressure tube was unsealed. The reaction mixture was allowed to warm with stirring to room temperature, was diluted with water, CH_2Cl_2 (10 mL) and THF (50 mL), and was washed with water followed by brine. The organic layer was dried over Na_2SO_4 and evaporated to dryness to afford **15** (94%) as a white solid: mp 234−240 °C (dec); TLC R_f = 0.23 (hexanes/EtOAc, 2:1); IR (KBr) 3310, 2976, 1708, 1372, 1291, 1169, 1116 cm^{-1}; ^{1}H NMR (200 MHz, $CDCl_3$) δ 1.63 (s, 9H), 8.08 (d, 2H, J = 8.0 Hz), 8.24 (d, 2H, J = 8.0 Hz); ^{13}C NMR (50 MHz, $CDCl_3$) δ 28.2, 81.5, 128.8, 135.4, 135.7, 165.7. Attempts to obtain a mass spectrum were unsuccessful.

4-(3-Nitrophenyl)-benzoic Acid *tert*-Butyl Ester (11a). A solution of 4-iodobenzoic acid *tert*-butyl ester **10a** (1.8 g, 5.9 mmol), 3-nitrobenzeneboronic acid (1.23 g, 7.4 mmol), tetrakis(triphenylphosphine)-palladium(0) (200 mg, 3 mol %), and 5 mL of 2 M aqueous Na_2CO_3 in toluene (150 mL) and ethanol (10 mL) was refluxed and stirred under a nitrogen atmosphere for 12 h. The reaction mixture was cooled to room temperature and partitioned between EtOAc (300 mL) and water (100 mL). The organic layer was washed with brine and dried over $MgSO_4$, and the solvent was removed under reduced pressure. Purification of the product by flash column chromatography afforded 1.66 g (94%) of **11a** as a white solid: mp 101−102 °C; TLC R_f = 0.29 (hexanes/EtOAc, 15:1); IR (KBr) 3008, 2984, 1701, 1531, 1350, 1303, 1161, 1122 cm^{-1}; ^{1}H NMR (200 MHz, $CDCl_3$) δ 1.62 (s, 9H), 7.64 (t, 1H, J = 8.0 Hz), 7.66 (d, 2H, J = 8.1 Hz), 7.93 (d, 1H, J = 7.8 Hz), 8.10 (d, 2H, J = 6.7 Hz), 8.23 (dd, 1H, J = 8.1, 1.1 Hz), 8.46 (m,1H); ^{13}C NMR (50 MHz, $CDCl_3$) δ 28.2, 81.4, 122.1, 122.7, 126.9, 129.9, 130.2, 132.0, 133.1, 141.8, 142.4, 148.7, 165.2; HRMS−FAB (M + Na^+) calcd for $C_{17}H_{17}NNaO_4$ 322.10558, found 322.10435.

3-(3-Nitrophenyl)-benzoic Acid *tert*-Butyl Ester (11b). The Suzuki coupling procedure was the same as described for **11a**. From 3-iodobenzoic acid *tert*-butyl ester **10b** (490 mg, 1.6 mmol) and 3-nitrobenzeneboronic acid (330 mg, 1.9 mmol) was obtained 540 mg (96%) of **11b** as a white solid after purification by flash column chromatography: mp 97−98 °C; TLC R_f = 0.34 (hexanes/EtOAc, 15:1); IR (KBr) 2978, 1713, 1528, 1350, 1299, 738 cm^{-1}; ^{1}H NMR (200 MHz, $CDCl_3$) δ 1.61 (s, 9H), 7.54 (t, 1H, J = 7.8 Hz), 7.62 (t, 1H, J = 7.9 Hz), 7.76 (ddd, 1H, J = 7.8, 1.9, 1.2 Hz), 7.93 (ddd, 1H, J = 7.8, 1.8, 1.1 Hz), 8.03 (dt, 1H, J = 7.7, 1.3 Hz), 8.20 (ddd, 1H, J = 8.2, 2.2, 1.1 Hz), 8.23 (t, 1H, J = 2.1 Hz), 8.46 (t, 1H, J = 2.1 Hz); ^{13}C NMR (50 MHz, $CDCl_3$) δ 28.2, 81.6, 121.9, 122.4, 128.1, 129.1, 129.4, 129.9, 131.0, 133.0, 133.1, 138.8, 142.0, 148.7, 165.3; HRMS−FAB (M + Na^+) calcd for $C_{17}H_{17}NNaO_4$ 322.10558, found 322.10635.

2-(3-Nitrophenyl)-benzoic Acid *tert*-Butyl Ester (11c). The Suzuki coupling procedure was the same as described for **11a**. From 2-iodobenzoic acid *tert*-butyl ester **10c** (800 mg, 2.6 mmol) and 3-nitrobenzeneboronic acid (530 mg, 3.2 mmol) was obtained 590 mg (75%) of **11c** as a white oil after purification by flash chromatography: TLC R_f = 0.30 (hexanes/EtOAc, 15:1); IR (neat): 3071, 2978, 2934, 1713, 1531, 1349, 1129 cm^{-1}; ^{1}H NMR (200 MHz, $CDCl_3$) δ 1.27 (s, 9H), 7.30 (dd, 1H, J = 7.8, 1.6 Hz), 7.40−7.68 (m, 4H), 7.88 (dd, 1H, J = 7.2, 1.6 Hz), 8.18 (br t, 1H, J = 1.9 Hz), 8.16−8.25 (m, 1H); ^{13}C NMR (50 MHz, $CDCl_3$) δ 27.7, 81.8, 121.9, 123.6, 128.2, 128.9, 130.3, 130.5, 131.2, 132.4, 134.7, 139.7, 143.6, 147.9, 166.9; HRMS−FAB (M + Na^+) calcd for $C_{17}H_{17}NO_4$ 322.10558, found 322.10492.

4-(4-Nitrophenyl)-benzoic Acid *tert*-Butyl Ester (11d). The Suzuki coupling procedure was the same as described for **11a**. From 4-carboxybenzeneboronic acid *tert*-butyl ester **15** (1.30 g, 6.0 mmol) and 4-iodonitrobenzene (2.24 g, 9.0 mmol) was obtained 1.5 g (84%) of **11d** as a white solid after purification by flash column chromatography (CH_2Cl_2/hexanes, 1:1): mp 173−174 °C; TLC R_f = 0.19 (hexanes/EtOAc, 20:1); IR (KBr) 2978, 2938, 1702, 1523, 1345, 1301, 1164, 1119, 848, 747 cm^{-1}; ^{1}H NMR (200 MHz, $CDCl_3$) δ 1.60 (s, 9H), 7.64 (d, 2H, J = 8.7 Hz), 7.74 (d, 2H, J = 9.0 Hz), 8.08 (d, 2H, J = 8.7 Hz), 8.29 (d, 2H, J = 9.0 Hz); ^{13}C NMR (50 MHz, $CDCl_3$) δ 28.2, 81.4, 124.2, 127.2, 128.0, 130.2, 132.3, 142.5, 146.5, 147.5, 165.2; HRMS−FAB (M + Na^+) calcd for $C_{17}H_{17}NNaO_4$ 322.10558, found 322.10462.

4-(3-Nitrosophenyl)-benzoic Acid *tert*-Butyl Ester (12a). To a solution of 4-(3-nitrophenyl)-benzoic acid *tert*-butyl ester **11a** (1.24 g, 4.15 mmol) in 2-methoxyethanol (25 mL) was added zinc dust (624 mg, 9.5 mmol) and ammonium chloride (363 mg, 6.8 mmol). The reaction mixture was stirred at room temperature for about 1 h while being monitored by TLC to minimize over-reduction of the hydroxyamine to the amine, which inevitably occurs to some extent. The crude hydroxylamine solution was cooled to 0 °C, $FeCl_3$ (2.0 g, 12.5 mmol) in 30 mL of H_2O/ethanol (5/1 v/v) was added, and the mixture was stirred for 3 h at 0 °C. The reaction mixture was extracted with EtOAc (3 × 40 mL), and the organic layers were combined, washed with brine, dried over $MgSO_4$, filtered, and concentrated under reduced pressure. To remove the small amount of anilinic byproduct present, the crude nitroso compound was purified quickly by flash column chromatography (hexanes/EtOAc, 25:1) to afford 1.01 g (86%) of **12a** as a green oil. Due to the instability of the nitroso compounds, they were generally used immediately, though in some cases they were stored briefly at −20 °C: TLC R_f = 0.33 (hexanes/EtOAc, 25:1); IR ($CHCl_3$) 3018, 2399, 1708, 1605, 1499, 1296, 1222, 748 cm^{-1}; ^{1}H NMR (200 MHz, $CDCl_3$) δ 1.62 (s, 9H), 7.64−7.72 (m, 3H), 7.91 (tm, 2H, J = 8.2 Hz), 8.07−8.11 (m, 3H); ^{13}C NMR (50 MHz, $CDCl_3$) δ 28.2, 81.3, 119.6, 120.2, 126.9, 129.9, 130.2, 131.8, 133.8, 141.5, 142.9, 165.3, 165.8; HRMS−FAB (M + H^+) calcd for $C_{17}H_{18}NO_3$ 284.12867, found 284.12933.

3-(3-Nitrosophenyl)-benzoic Acid *tert*-Butyl Ester (12b). The procedure was the same as for **12a**; from 260 mg (0.87 mmol) of nitro compound **11b** in 10 mL of 2-methoxyethanol was obtained 210 mg (85%) of **12b** as a green oil: TLC R_f = 0.31 (hexanes/EtOAc, 25:1); IR ($CHCl_3$) 2982, 2253, 1709, 1369 cm^{-1}; ^{1}H NMR (200 MHz, $CDCl_3$) δ 1.62 (s, 9H), 7.53 (t, 1H, J = 7.8 Hz), 7.68 (t, 1H, J = 7.8 Hz), 7.79 (dt, 1H, J = 7.8, 1.3 Hz), 7.88 (dt, 1H, J = 7.9, 1.3 Hz), 7.95 (dt, 1H, J = 7.6, 1.3 Hz), 8.03 (dt, 1H, J = 7.7, 1.2 Hz), 8.10 (t, 1H, J = 1.8 Hz), 8.27 (t, 1H, J = 1.8 Hz);^{13}C NMR (50 MHz, $CDCl_3$) δ 28.2, 81.4, 119.5, 120.0, 128.1, 129.0, 129.2, 129.9, 131.0, 132.9, 133.7, 139.3, 141.7, 165.3, 165.9; HRMS−FAB (M + H^+) calcd for $C_{17}H_{18}NO_3$ 284.12867, found 284.12768.

2-(3-Nitrosophenyl)-benzoic Acid *tert*-Butyl Ester (12c). The procedure was the same as for **12a**; from 600 mg (2.0 mmol) of nitro compound **11c** in 20 mL of 2-methoxyethanol was obtained 440 mg (78%) of **12c** as a green oil: TLC R_f = 0.33 (hexanes/EtOAc, 15:1); IR ($CHCl_3$) 2982, 2254, 1710, 1254, 1162 cm^{-1}; ^{1}H

NMR (200 MHz, $CDCl_3$) δ 1.25 (s, 9H), 7.30−8.30 (m, 8H); ^{13}C NMR (50 MHz, $CDCl_3$) δ 27.6, 81.6, 120.3, 120.4, 128.0, 128.9, 130.3, 130.5, 131.2, 132.6, 135.5, 140.2, 143.4, 165.5, 167.2; HRMS−FAB (M + Na^+) calcd for $C_{17}H_{17}NNaO_3$ 306.1106, found 306.11167.

4-(4-Nitrosophenyl)-benzoic Acid *tert*-Butyl Ester (12d). The procedure was the same as for **12a**; from 300 mg (1.0 mmol) of nitro compound **11d** in 10 mL of 2-methoxyethanol was obtained 230 mg (81%) of **12d** as a green solid: TLC R_f = 0.36 (hexanes/CH_2Cl_2, 1:1); IR ($CHCl_3$) 3055, 2984, 2312, 2260, 1709, 1297 cm^{-1}; ^{1}H NMR (200 MHz, $CDCl_3$) δ 1.61 (s, 9H), 7.68 (d, 2H, J = 8.2 Hz), 7.82 (d, 2H, J = 8.3 Hz), 7.97 (d, 2H, J = 8.3 Hz), 8.09 (d, 2H, J = 8.2 Hz); ^{13}C NMR (50 MHz, $CDCl_3$) δ 28.2, 81.4, 121.5, 127.3, 128.1, 130.1, 131.3, 142.9, 146.9, 164.7, 165.2; HRMS−FAB (M + Na^+) calcd for $C_{17}H_{17}NNaO_3$ 306.1106, found 306.11129.

General Procedure for Preparation of Fmoc-Abc-O*t*-Bu Isomers (13a−d). The indicated amounts of amine and nitroso compound were combined in glacial acetic acid and stirred at room temperature for 24 h. The solvent was removed in vacuo, and the residue was purified by flash chromatography with 4:1 hexanes/EtOAc for mxAbc derivatives **13a**−**c** or with 50:1 $CHCl_3$/hexanes for the ppAbc derivative **13d**. In all cases, the fractions containing the well-separated *cis* and *trans* isomers were combined. NMR data are reported for the *trans* isomer of each compound.

[1,1′-Biphenyl]-4-carboxylic Acid, 3′-[[4′-[[[(9*H*-Fluoren-9-ylmethoxy)carbonyl] amino]methyl][1,1′-biphenyl]-3-yl]azo], 1,1-Dimethylethyl Ester (Fmoc-mpAbc-O*t*-Bu, 13a). From 1.20 g (2.9 mmol) of amine **9a** and 810 mg (2.9 mmol) of nitroso compound **12a** in 50 mL of AcOH was obtained 1.69 g (86%) of **13a** as a yellow oil: TLC R_f = 0.24 (*trans*), 0.15 (*cis*) (hexanes/EtOAc, 4:1); IR (CCl_4) 3461, 3023, 2984, 2940, 2906, 1745, 1373, 1240, 776 cm^{-1}; ^{1}H NMR (300 MHz, $CDCl_3$) δ 1.64 (s, 9H), 4.24 (t, 1H, J = 6.7 Hz), 4.44 (d, 2H, J = 6.0 Hz), 4.49 (d, 2H, J = 6.9 Hz), 5.26 (br s, 1H), 7.27−7.44 (m, 6H), 7.56−7.80 (m, 12H) 7.94 (br d, 1H, J = 8.1 Hz), 7.97 (dt, 1H, J = 8.4, 1.8 Hz) d, 8.11 (d, 2H, J = 8.4, 1.2 Hz), 8.18 (br s, 1H), 8.22 (t, 2H, J = 1.8 Hz); ^{13}C NMR (50 MHz, $CDCl_3$) δ 28.3, 44.8, 47.3, 66.7, 81.2, 120.0, 121.7, 121.8, 122.4, 125.0, 127.0, 127.1, 127.5, 127.7, 128.1, 129.6, 129.7, 130.1, 131.2, 138.1, 139.5, 141.2, 141.4, 141.8, 143.9, 144.2, 153.0, 153.1, 156.5, 165.6; HRMS−FAB (M + Na^+) calcd for $C_{45}H_{39}N_3NaO_4$ 708.28383, found 708.28437.

[1,1′-Biphenyl]-3-carboxylic Acid, 3′-[[3′-[[[(9*H*-Fluoren-9-ylmethoxy)carbonyl] amino]methyl][1,1′-biphenyl]-3-yl]azo], 1,1-Dimethylethyl Ester (Fmoc-mmAbc-O*t*-Bu, 13b). From 128 mg (0.28 mmol) of amine **9b** and 80 mg (0.28 mmol) of nitroso compound **12b** in 5 mL of AcOH was obtained 150 mg (78%) of **13b** as a yellow oil: TLC R_f = 0.25 (*trans*), 0.15 (*cis*) (hexanes/EtOAc, 4:1); IR (CCl_4) 3452, 2981, 2929, 2856, 2322, 1717, 1549, 1512, 1264, 1218, 776 cm^{-1}; ^{1}H NMR (300 MHz, $CDCl_3$) δ 1.63 (s, 9H), 4.23 (t, 1H, J = 6.8 Hz), 4.36−4.49 (m, 4H), 5.20 (br s, 1H), 7.26−7.33 (m, 3H), 7.37 (t, 2H, J = 7.2 Hz), 7.45 (t, 1H, J = 7.8 Hz), 7.52 (t, 1H, J = 7.8 Hz), 7.56−7.65 (m, 5H), 7.73 (t, 2H, J = 7.8 Hz), 7.69−7.78 (m, 2H), (7.84 (ddd, 1H, J = 7.8, 1.8, 1.2 Hz), 7.946 (dt, 1H, J = 7.8, 1.2 Hz), 7.950 (dt, 1H, J = 7.8, 1.5 Hz), 8.01 (dt, 1H, J = 7.8, 1.4 Hz), 8.19 (t, 1H, J = 1.7 Hz), 8.22 (t, 1H, J = 1.8 Hz), 8.33 (t, 1H, J = 1.5 Hz); ^{13}C NMR (50 MHz, $CDCl_3$) δ 28.2, 45.1, 47.3, 66.8, 81.3, 120.0, 121.7, 121.8, 121.9, 122.1, 125.0, 126.5, 126.9, 127.1, 127.7, 128.2, 128.7, 128.8, 129.3, 129.6, 129.66, 129.72, 129.8, 130.0, 131.2, 132.7, 139.1, 140.5, 140.8, 141.3, 141.4, 141.9, 143.9, 153.05, 153.09, 156.5, 165.7; HRMS−FAB (M + Na^+) calcd for $C_{45}H_{39}N_3NaO_4$ 708.28383, found 708.28442.

[1,1′-Biphenyl]-2-carboxylic Acid, 3′-[[2′-[[[(9*H*-Fluoren-9-ylmethoxy)carbonyl] amino]methyl][1,1′-biphenyl]-3-yl]azo], 1,1-Dimethylethyl Ester (Fmoc-moAbc-O*t*-Bu, 13c). From 150 mg (0.36 mmol) of amine **9c** and 105 mg (0.36 mmol) of nitroso compound **12c** in 7 mL of AcOH was obtained 200 mg (80%) of **13c** as a yellow oil: TLC R_f = 0.26 (*trans*), 0.16 (*cis*) (hexanes/EtOAc, 4:1); IR (CCl_4) 3454, 3067, 2979, 2930, 2359, 1729, 1549, 1509, 1247, 776 cm^{-1}; ^{1}H NMR (300 MHz, $CDCl_3$) δ 1.25 (s, 9H), 4.17 (t, 1H, J = 6.9 Hz), 4.38 (d, 2H, J = 7.2 Hz), 4.41 (d, 2H, J = 7.2 Hz), 5.00 (t, 1H, J = 5.9 Hz), 7.10−7.60 (m, 17H), 7.74 (d, 2H, J = 7.2 Hz), 7.85 (dd, 1H, J = 7.7, 1.4 Hz), 7.87−7.97 (m, 4H); ^{13}C NMR (50 MHz, $CDCl_3$) δ 27.6, 42.9, 47.3, 66.7, 81.4, 119.9, 122.2, 122.4, 122.5, 123.1, 125.0, 127.1, 127.5, 127.6, 127.7, 128.2, 128.5, 128.7, 129.2, 130.0, 130.6, 130.9, 131.4, 131.6, 132.8, 135.7, 140.7, 141.3, 141.7, 143.0, 143.9, 152.2, 152.6, 156.4, 167.8; HRMS−FAB (M + Na^+) calcd for $C_{45}H_{39}N_3NaO_4$ 708.28383, found 708.28360.

[1,1′-Biphenyl]-4-carboxylic Acid, 4′-[[4′-[[[(9*H*-Fluoren-9-ylmethoxy)carbonyl] amino]methyl][1,1′-biphenyl]-4-yl]azo], 1,1-Dimethylethyl Ester (Fmoc-ppAbc-O*t*-Bu, 13d). From 140 mg (0.33 mmol) of amine **9d** and 95 mg (0.33 mmol) of nitroso compound **12d** in 5 mL of AcOH was obtained 194 mg (85%) of **13d** as a pale orange solid (mp 202−204 °C, dec after 210 °C): TLC R_f = 0.21 (*trans*), 0.10 (*cis*) ($CHCl_3$/hexanes, 50:1); IR (KBr) 3388, 2361, 2345, 1724, 1689, 1521, 1301, 1224 cm^{-1}; ^{1}H NMR (300 MHz, $CDCl_3$) δ 1.64 (s, 9H), 4.24 (t, 1H, J = 6.6 Hz), 4.44 (d, 2H, J = 5.8 Hz), 4.48 (d, 2H, J = 6.7 Hz), 5.15 (br t, 1H, J = 5.8 Hz), 7.31 (t, 2H, J = 7.2 Hz), 7.35−7.44 (m, 4H), 7.61 (d, 2H, J = 8.7 Hz), 7.64 (d, 2H, J = 8.1 Hz), 7.68−7.82 (m, 8H), 8.026 (d, 2H, J = 8.4 Hz), 8.034 (d, 2H, J = 8.7 Hz), 8.08 (d, 2H, J = 8.7 Hz); ^{13}C NMR (50 MHz, $CDCl_3$) δ 28.2, 44.5, 47.3, 66.7, 81.2, 120.0, 123.5, 125.0, 126.9, 127.1, 127.5, 127.6, 127.7, 127.9, 128.1, 130.0, 131.3, 138.2, 139.4, 141.3, 142.6, 143.3, 143.9, 144.0, 151.9, 152.3, 165.5; HRMS−FAB (M + Na^+) calcd for $C_{45}H_{39}N_3NaO_4$ 708.28383, found 708.28403.

[1,1′-Biphenyl]-4-carboxylic Acid, 3′-[[4′-[[[(9*H*-Fluoren-9-ylmethoxy)carbonyl] amino]methyl][1,1′-biphenyl]-3-yl]azo] (Fmoc-mpAbc-OH). Fmoc-mpAbc-O*t*-Bu **13a** (200 mg, 29.2 mmol) was dissolved in 10 mL of TFA/H_2O (95:5) and stirred at room temperature for 2 h. The product was evaporated to dryness in vacuo, suspended in ether, and collected by filtration to afford 156 mg (85%) of the desired product as a yellow solid: ^{1}H NMR (200 MHz, DMSO-d_6) δ 4.16−4.25 (m, 1H), 4.24 (d, 2H, J = 6.1 Hz), 4.36 (d, J = 6.7 Hz), 7.26−7.46 (m, 6H), 7.64−7.78 (m, 6H), 7.83−8.00 (m, 9H), 8.06 (d, 2H, J = 8.1 Hz), 8.19 (br s, 1H), 8.26 (br s, 1H); ^{13}C NMR (50 MHz, DMSO-d_6) δ 43.4, 46.7, 65.3, 120.0, 120.9, 121.1, 121.3, 122.0, 125.1, 126.7, 127.0, 127.5, 127.7, 129.7, 129.8, 130.0, 130.1, 130.2, 137.6, 139.6, 140.3, 140.7, 141.2, 143.2, 143.8, 152.4, 156.3, 167.0; LRMS−FAB (M + H^+) calcd for $C_{41}H_{32}N_3O_4$ 630, found 630 (FAB). Efforts to obtain a high-resolution mass spectrum were unsuccessful.

Synthesis of Model Peptide STPPK(mpAbc)KKRKV. All amino acids had N_α-Fmoc protection and side chain protecting groups as follows: *t*-Bu for Ser and Thr, Boc for Lys, and 2,2,5,7,8-pentamethyl-chroman-6-sulfonyl (Pmc) for Arg. Synthesis was performed manually using a Burrell wrist-action shaker and a glass reaction vessel derived from a fritted glass Büchner funnel by the addition of a threaded top and a Teflon stopcock in the stem. Fmoc-valyl Wang resin (125 mg, 0.80 mmol/g) was swelled by shaking in 5 mL of NMP for 30 min and drained by suction. Cycles of deprotection and synthesis were performed as follows. Deprotection was effected by shaking the resin for 15−20 min in 5 mL of 20% (v/v) piperidine in NMP; the deprotection cocktail was removed by suction, and the resin was rinsed by shaking for 5 min each with 5−10 mL portions of NMP (3×) and 2-propanol (3×). Coupling: to 0.2 mmol of protected amino acid in 0.8 mL of NMP in the reaction vessel was added PyBOP (0.2 mmol in 0.4 mL of NMP), 1-hydroxybenzotriazole (HOBt, 0.2 mmol in 0.4 mL of NMP), and DIPEA (0.4 mmol, 66 μL); the mixture was shaken for 2 h, drained, and washed with 5−10 mL portions of NMP (6×). For mpAbc, 0.15 mmol of protected amino acid with proportionate amounts of other reaction components and a coupling time of 3 h were employed.

Deprotection and cleavage were performed on 30% of the resin with 1 mL of 95:5 (v/v) TFA/water for 2 h at room temperature

with periodic agitation. After collection of the liquid by suction, the resin was rinsed with TFA (3 × 1 mL), the rinsings were combined with the reaction mixture, and the bulk of the TFA was removed by rotary evaporation. The residue was partitioned between water (10 mL) and ether (10 mL), the ether layer was extracted with an equal volume of water, and the combined aqueous layers were lyophilized. Purification of the product by reversed-phase HPLC was performed on a Waters Delta-Pak C18 column (25 mm × 100 mm) at a flow rate of 10 mL/min with a two-segment linear gradient as follows (A = 0.1% TFA in water, B = 0.08% TFA in CH_3CN): 0 min, 0% B; 5 min, 20% B; 35 min, 40% B. Under these conditions, the more polar *cis* isomer elutes at 14 min, and the less polar *trans* isomer elutes at 21 min. The composition of the product was verified by MALDI-TOF mass spectrometry: LRMS−FAB ($M + H^+$) calcd for $C_{78}H_{117}N_{20}O_{14}$ 1,557.9, found 1,557.7.

Quantitative Fmoc Analysis. Samples (ca. 10 mg) of the resin-bound peptides were thoroughly washed (3× with NMP and 3× with CH_2Cl_2 in addition to the standard post-coupling rinses), dried in vacuo, weighed, and treated with 1 mL of 20% piperidine in NMP for 20 min with periodic agitation. The absorbance at 301 nm of the deprotection cocktail was measured after 1:50 dilution with NMP, and the concentration was determined using $\epsilon_{301} = 7800$ $M^{-1}cm^{-1}$ for the piperidine-dibenzofulvene adduct. Yields were calculated from concentration with correction for theoretical mass addition at each step.

Acknowledgment. Substantial portions of this project were conducted at Texas A&M University. For financial support, we thank MarineBio21, Ministry of Maritime Affairs and Fisheries, Korea (MOMAF, to S.B.P.), the Korean Science and Engineering Foundation (KOSEF, to S.B.P.), the Robert A. Welch Foundation (A-1332 to R.F.S.), the National Institute of General Medical Sciences (GM 57543 to R.F.S.), Texas A&M University, and the Laboratory Directed Research and Development Program of Oak Ridge National Laboratory, managed by UT-Battelle, LLC, for the U.S. Department of Energy under contract no. DE-AC05-00OR22725. For mass spectral analyses, we thank the Mass Spectrometry Applications Laboratory of Texas A&M University.

Supporting Information Available: General experimental procedures, ^1H NMR spectra for all compounds, ^{13}C NMR spectrum for compounds **13a**−**c** and **14**, and coordinates for all molecular mechanics structures. This material is available free of charge via the Internet at http://pubs.acs.org.

JO060763Q